Late Quaternary eolian and alluvial response to paleoclimate, Canyonlands, southeastern Utah

Marith C. Reheis[†]
Richard L. Reynolds
Harland Goldstein
U.S. Geological Survey, MS-980, Federal Center, Box 25046, Denver, Colorado 80225, USA

Helen M. Roberts
Institute of Geography and Earth Sciences, University of Wales, Aberystwyth SY23 3DB, Wales, UK

James C. Yount
U.S. Geological Survey, MS-980, Federal Center, Box 25046, Denver, Colorado 80225, USA

Yarrow Axford
Institute of Arctic and Alpine Research, University of Colorado, Boulder, Colorado 80309, USA

Linda Scott Cummings
Paleo Research Institute, 2675 Youngfield Street, Golden, Colorado 80401, USA

Nancy Shearin
Bureau of Land Management, Monticello Field Office, Monticello, Utah 84535, USA

ABSTRACT

In upland areas of Canyonlands National Park, Utah, thin deposits and paleosols show late Quaternary episodes of eolian sedimentation, pedogenesis, and climate change. Interpretation of the stratigraphy and optically stimulated luminescence ages of eolian and nearby alluvial deposits, their pollen, and intercalated paleosols yields the following history: (1) Eolian deposition at ca. 46 ka, followed by several episodes of alluviation from some time before ca. 40 ka until after 16 ka (calibrated). (2) Eolian deposition from ca. 17 ka to 12 ka, interrupted by periods of pedogenesis, coinciding with late Pleistocene alluviation as local climate became warmer and wetter. (3) A wetter period from 12 to 8.5 ka corresponding to the peak of summer monsoon influence, during which soils formed relatively quickly by infiltration of eolian silt and clay, and trees and grasses were more abundant. (4) A drier period between ca. 8.5 and 6 ka during which sheetwash deposits accumulated and more desertlike vegetation was dominant; some dunes were reactivated at ca. 8 ka. (5) Episodic eolian and fluvial deposition during a wetter, cooler period that began at ca. 6 ka and ended by ca. 3–2 ka, followed by a shift to drier modern conditions; localized mobilization of dune sand has persisted to the present. These interpretations are similar to those of studies at the Chaco dune field, New Mexico, and the Tusayan dune field, Arizona, and are consistent with paleoclimate interpretations of pollen and packrat middens in the region.

A period of rapid deposition and infiltration of eolian dust derived from distant igneous source terranes occurred between ca. 12 and 8 ka. Before ca. 17 ka, and apparently back to at least 45 ka, paleosols contain little or no such infiltrated dust. After ca. 8 ka, either the supply of dust was reduced or the more arid climate inhibited translocation of dust into the soils.

Keywords: Colorado Plateau, dunes, eolian dust, paleoclimate, paleosols, soil nutrients.

INTRODUCTION

Semiarid and arid regions of the world react sensitively to climate change. Indicators of environmental change commonly used in studies of these areas include lacustrine deposits, pollen from stratigraphic sequences, and plant macrofossils from packrat middens. Eolian sand sheets and dunes are common features of semiarid regions, and their deposits and intercalated paleosols potentially contain a long-term record of landscape response to climate fluctuations.

Mineral dust may strongly influence landscapes and ecosystems by adding materials to soils that change their properties (e.g., Reheis et al., 1995; Simonson, 1995; Herrmann et al., 1996). Dust incorporated into aridic soils affects water-infiltration rates, the evolution and stability of desert surfaces, the distribution of surface and subsurface water (McFadden et al., 1987, 1998; McDonald et al., 1996), and relations among eolian dust, distribution of plants and soil crust, rain-water runoff, and productivity (McFadden and McAuliffe, 1997; Shachak and Lovett, 1998; Belnap et al., 2000; Reynolds et al., 2001).

The Canyonlands physiographic section of the Colorado Plateau (Fig. 1) is characterized by high-elevation (1500–2200 m) benches, mesas, and slickrock buttes of resistant sandstone. These landforms, in many cases isolated from alluvial and colluvial sedimentation, are commonly mantled by a thin layer of fine-grained sandy sediment supporting upland grass and shrub steppe. Active wind transport of sand occurs in areas of abundant sand supply and where vegetation has been disturbed by land use. Layers of locally derived eolian sand separated by

[†]E-mail: mreheis@usgs.gov.

GSA Bulletin; July/August 2005; v. 117; no. 7/8; p. 1051–1069; doi: 10.1130/B25631.1; 10 figures; 4 tables; Data Repository item 2005106.

paleosols in small relict dune fields indicate late Quaternary changes in land-surface stability.

In this paper, we discuss the depositional history, age, and paleoclimate setting of eolian and alluvial deposits and intercalated paleosols at five sites in the area of Canyonlands National Park, Utah. The relatively thin deposits of eolian sand preserve a nearly 50 k.y. record of alternating periods of deposition and stability. In combination with pollen contained in these deposits, these records provide new insights on the late Quaternary landscape stability and paleoclimate of the Colorado Plateau. In addition, textural and magnetic data record episodic additions of far-traveled infiltrated dust in surface and buried soils, with ecologic implications for modern ecosystem dynamics in this area.

STUDY SITES AND METHODS

The Canyonlands area of the Colorado Plateau is cool and semiarid. At the Needles visitor center (Fig. 1), intermediate in location and altitude (1523 m) between four of our sites, mean annual precipitation is 21 cm (38 yr record), and mean January and July temperatures are –1.9 °C and 25.8 °C, respectively (National Climatic Data Center, http://www.wrcc.sage.dri.edu/climsum.html). The Neck station in the Island in the Sky district is 14 km from the northern study site (ISKY dune) and at the same altitude (1807 m). Precipitation and temperature ranges are similar to The Needles despite the difference in altitude. In both areas, ~40% of precipitation falls during late July to October, the remainder being about equally distributed through the year; prevailing winds are from the west.

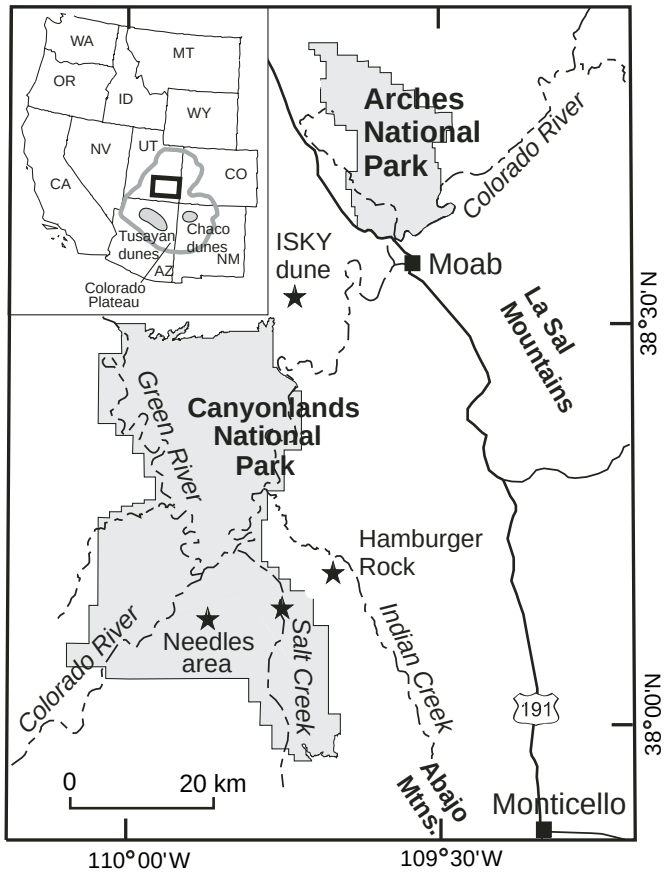

Figure 1. Maps of Canyonlands area and locations of study sites ("Needles area" includes Virginia Park and graben-fill sites). Inset, location of Canyonlands area (black box) within the Colorado Plateau and nearby dune fields. Mtns.—Mountains.

Study Sites

Virginia Park, the focus of most of our work (Fig. 1), is a sheltered basin of vegetated, stabilized sand dunes bordered on three sides by vertical sandstone cliffs, and on the fourth by a canyon (Fig. 2, Table 1). Dune ridges rise as much as 5 m above intervening swales. Auger holes indicate the sand is at least 4 m thick, thinning to zero at the margins. Modern vegetation includes abundant grasses and shrubs and scattered trees in bedrock and cliff-marginal locations (Table 1; M. Miller, U.S. Geological Survey, personal commun., 1998). Small drainages dissect the Quaternary sediment within the basin and locally provide exposures of the stratigraphy.

The Hamburger Rock site (Fig. 1, Table 1) has a thin sheet of Quaternary eolian sand, including active coppice dunes overlying shale. The Bureau of Land Management excavated trenches in the sand and underlying bedrock and in an adjacent area of sandy sheetwash alluvium in search of subsurface archaeological features. As part of this study, Shearin et al. (2000) described and sampled surface and buried soils and analyzed pollen samples from the sediment.

The ISKY site is a quarry in a partially active clifftop dune containing paleosols on the eastern edge of the plateau between the Green and Colorado Rivers (Figs. 1 and 3A; Table 1). The Quaternary dune sand is probably derived from erosion of the nearby Navajo Sandstone (Huntoon et al., 1982). The graben-fill site (Figs. 2 and 3B; Table 1) east of Virginia Park contains deposits within a closed depression formed by faulting due to flow of underlying salt beds westward toward the Colorado River (Fig. 1; Hunt, 1969; Walsh and Schultz-Ela, 2003). Later incision by Chesler Canyon has created a near-vertical cut exposing more than 6 m of slightly gravelly, poorly sorted, silty sand with interbedded paleosols (Fig. 3B).

Salt Creek is an intermittently flowing tributary of the Colorado River that heads in the Abajo Mountains (Fig. 1). The modern sediment transported by Salt Creek includes fine to medium volcanic gravel from the Abajo Mountains and sand derived locally from the Cedar Mesa Sandstone. We studied five terrace surfaces flanking Salt Creek (Fig. 4).

Sampling and Description

Within Canyonlands National Park, stratigraphic descriptions and samples were primarily obtained with a soil auger, supplemented by natural exposures of dune sand and alluvium in arroyo cuts and by two shallow hand-dug soil pits (VP-1, VP-2; Fig. 2) in a dune crest and a dune swale. Outside the boundary of the park, samples were collected from backhoe pits at Hamburger Rock (Fig. 1; Shearin et al., 2000) and from a 9-m-thick section of dune sands and paleosols exposed by the quarry at ISKY dune. Most of the outcrops and soil pits were described (Table 2) following Birkeland (1999). The soil-auger sequences were

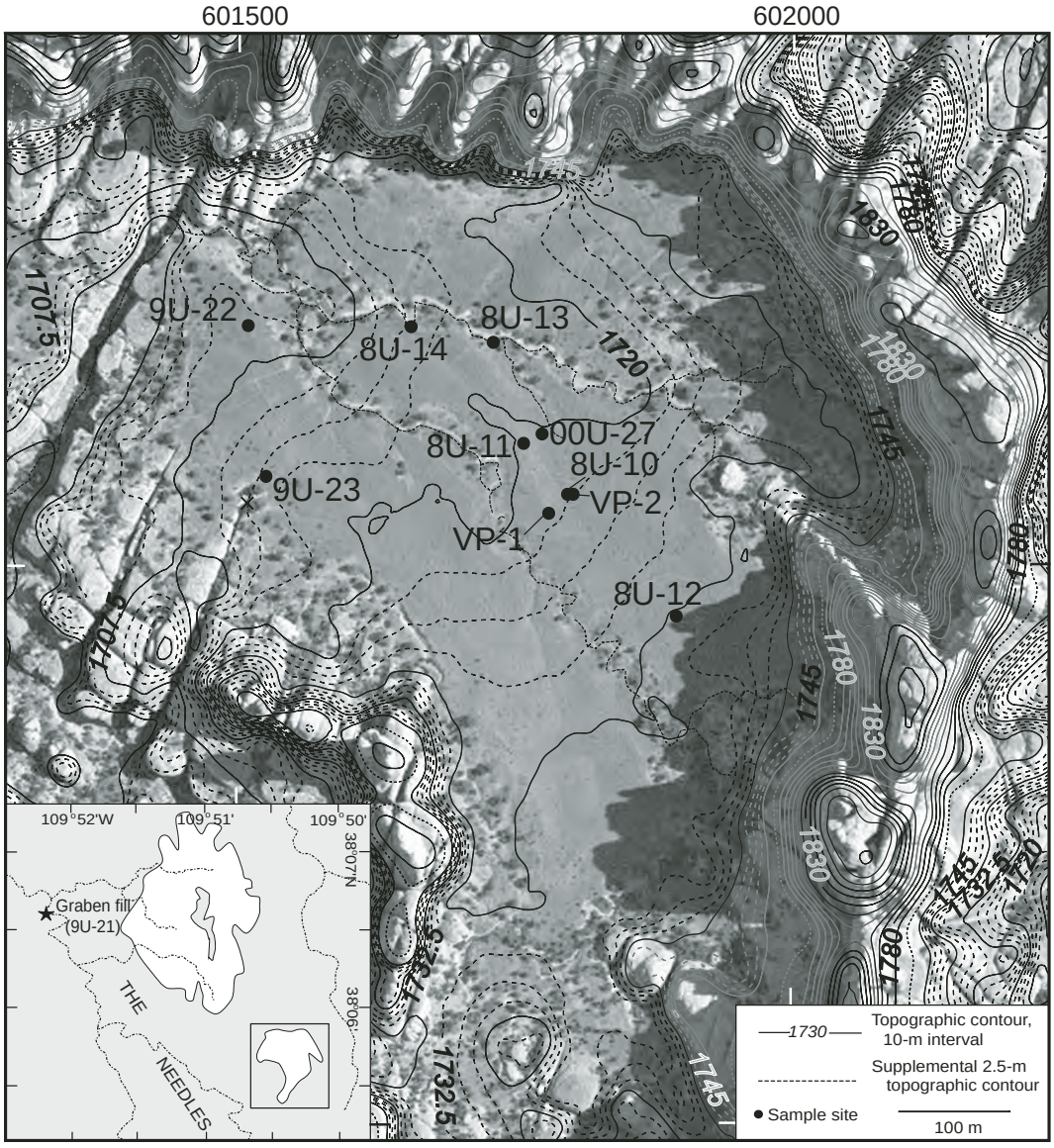

Figure 2. Location of Virginia Park and graben-fill site (inset), and map and sample locations in Virginia Park. Note subdued dune crests indicated by lighter tone and contours near 8U-11 and VP-1 (Table 1). Map constructed by using an aerial photo base with superimposed contours from digital elevation model, supplemented with detailed altitudes and survey points collected with a Trimble GPS unit and differentially corrected after processing.

TABLE 1. CHARACTERISTICS OF STUDY SITES IN THE CANYONLANDS AREA

Site name (altitude)	Sample designations	Substrate	Vegetation
Virginia Park (1720 m)	VP-1, VP-2 (pits) 8U-14, 8U-13 (arroyo cuts) 8U-10, 8U-11, 8U-12, 9U-22, 9U-23, 00U-27 (auger holes)	Dune sand overlying Cedar Mesa Formation (Billingsley et al., 2002)	Poaceae (grasses), *Bromus tectorum* (cheat grass), *Pinus edulis* (pinyon pine), *Juniperus osteosperma* (Utah juniper), *Atriplex canescens* (four-wing saltbush), *Ceratoides lanata* (winterfat), *Ephedra* (Mormon tea), *Plantago patagonica* (wooly plantain), *Artemisia tridentata* (big sagebrush), *Opuntia* spp. (prickly pear)
Hamburger Rock (1485 m)	Trenches 2, 3, 5, and 7	Eolian sand overlying Permian shale (Huntoon et al., 1982)	*A. canescens*, *Sarcobatus vermiculatus* (greasewood), *Ephedra*, *Tetradymia glabrata* (horsebush), *Gutierrezia sarothrae* (snakeweed), *Opuntia*, Poaceae, scattered *Juniperus*
ISKY dune (1807 m)	02U-1	Eolian sand overlying Kayenta Formation	Similar to Virginia Park but more *Pinus* and *Juniperus*
Graben fill (1585 m)	9U-21	Graben-fill deposits	Similar to Virginia Park
Salt Creek (1525 m)	SC-15	Alluvium	*A. canescens, S. vermiculatus, Salix exigua* (willow), *Tamarix ramosissima* (tamarisk), *Chrysothamnus nauseous* (rubber rabbitbrush), *A. tridentata*, Poaceae

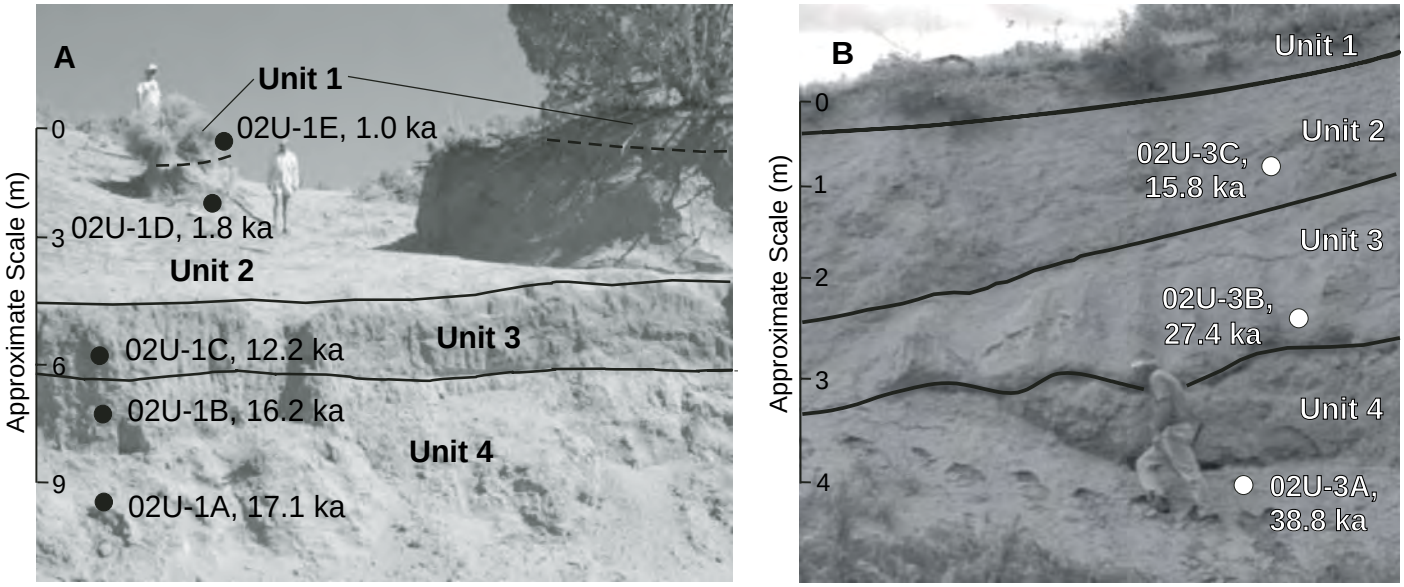

Figure 3. Photographs of selected study sites. Dots show locations and ages of optically stimulated luminescence (OSL) samples (02U-1A, etc.; Table 4 and Fig. DR1 [see footnote 1]). (A) Clifftop dune (ISKY site) on eastern edge of mesa top north of Canyonlands National Park. Sand pit exposes four eolian sand units separated by paleosols. (B) Graben-fill site east of Virginia Park (Fig. 2). Arroyo cut exposes one eolian (unit 1) and three alluvial units separated by paleosols.

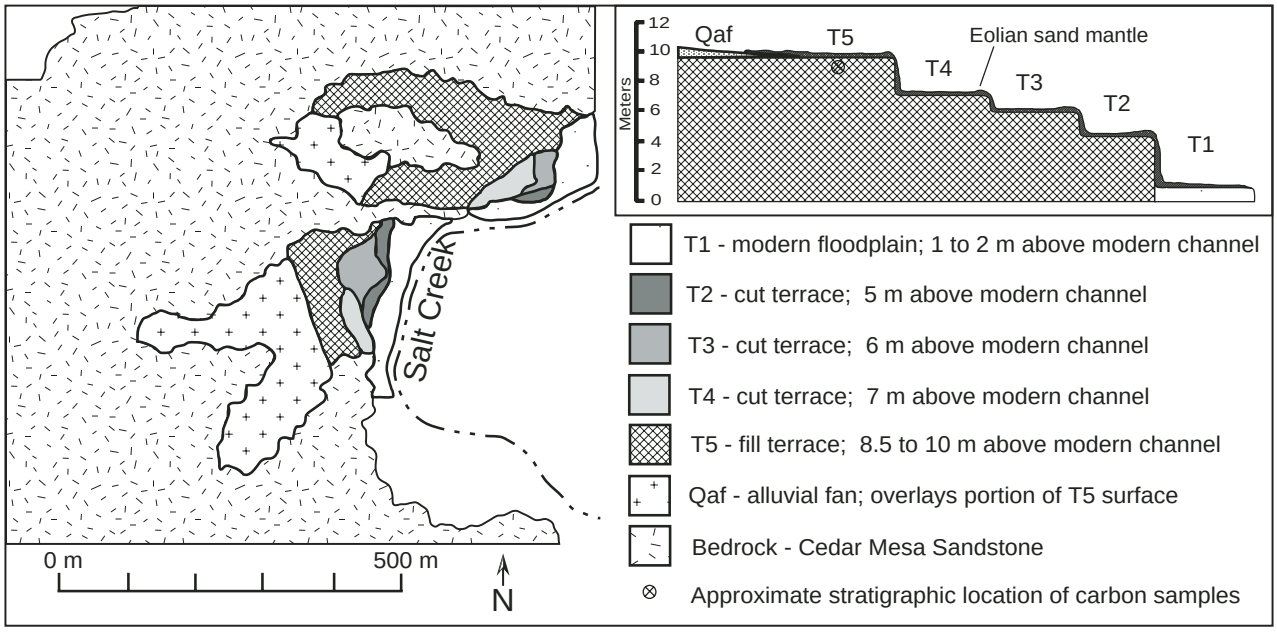

Figure 4. Map and generalized cross section of alluvial deposits along a portion of Salt Creek (location on Fig. 1).

described similarly, but with less precision because of the lack of visible exposure and because of the mixing that occurred when the auger was reinserted into the hole. Approximate soil horizon boundaries were identified during the augering by changes in soil color, carbonate morphology, effervescence in HCl, and sediment texture. Samples from the auger holes were taken from the interior of the largest, most intact clods of material within each bucketful. Laboratory results from these samples are plotted as single points with depth, in contrast to the depth-integrated samples obtained from outcrops and soil pits.

Particle Size and Magnetic Analyses

Particle-size distribution of samples was determined as volume percentage by a laser-light scattering method (McCave and Syvitski, 1991). Particle-size distributions measured in this way should be similar to those measured by conven-

TABLE 2. SELECTED SOIL DESCRIPTIONS AND LABORATORY DATA

Horizon[‡]	Depth (cm)	Dry color	Moist color	Structure[§]	Dry consistence[#]	Clay films[††]	Stage $CaCO_3$[‡], other cements[‡‡]	$CaCO_3$ (%)	Silt (%)	Clay (%)
VP-1, hand-dug soil pit in dune crest, Virginia Park site										
A	0–6	7.5YR7/4	7.5YR5/4	2m sbk, 1fpl	so	0	0, no eff.	4.63	23.84	5.36
Bwk	6–19	5YR6/5	5YR4/6	2m-c sbk	so	0	0, es	6.21	28.43	9.16
B1tk	19–30	5YR7/5	5YR5/6	2f-m sbk	so	1nbr	0, es	6.32	26.09	8.27
Bt2k	30–55	5YR6/6	5YR4/8	2f-m sbk	so	2nbr, 1npo, 1npf	I, es	7.77	18.60	6.22
B31tkb	55–66	5YR6/5	5YR5/6	2f-m abk	sh	1npf	I+, ev	7.02	28.36	8.22
B32tkb	66–78	5YR6/4	5YR5/6	2f-m abk	h	2npf	III, ev	7.02	28.20	7.83
Bkb	78–90	n.d.	n.d.	n.d.	h	n.d.	III, ev	14.59	15.48	4.39
8U-11, auger hole in dune crest near VP-1, Virginia Park site										
A/Bw	0–22	5YR6/5	5YR4/6	2f-m sbk	so	0	0, e-es	7.38	23.99	7.38
Bw[†]	22–50	5YR6/5	5YR5/6	2f-m sbk	so-sh	0	0-I, es-ev	1.29	27.13	9.27
Btk1b1[†]	50–86	5YR6/6	5YR5/6	2f-m sbk	sh-h	0	I+, ev	2.27	24.73	7.07
Btk2b1[†]	86–118	5YR7/4	5YR6/5	3f-m sbk	h	0	II+, ev	5.98	20.56	6.48
Bkb1[†]	118–151	5YR7/4	5YR5/6	2f-m sbk	sh-h	0	II, ev	3.95	13.74	3.16
Bkb2[†]	151–172	5YR7/5	5YR6/6	n.d.	sh-so	0	I, es-ev	1.88	17.18	5.60
Ckb2[†]	172–251	5YR7/5	5YR6/6	Single grain	lo-so	0	I, es-ev	3.36	20.93	6.12
Cyb2[†]	251–278	5YR7/5	5YR6/6	Single grain	lo-so	0	0, es; gypsum rosettes	3.74	17.84	6.24
VP-2, hand-dug soil pit in dune swale, Virginia Park site										
Ak	0–5	5YR6/4	5YR4/4	1f-m sbk	so	0	0, e	5.86	29.41	5.79
Bw	5–14	5YR6/5	5YR4/6	1f cr	so	0	0, e-	7.19	31.04	8.89
Bwk	14–44	5YR6/5	5YR5/6	2f-m sbk	so-sh	0	I, e-es	7.10	26.46	7.65
Btk1b	44–55	5YR7/4	5YR5/6	2f-m sbk	sh	1nbr	II, ev	7.04	23.71	7.60
Btk2b	55–85	5YR6/5	5YR5/6	2m-c abk	sh	1nbr, 1npf	I, es	7.67	28.55	10.03
Bkb	98–115	n.d.	n.d.	n.d.	h	n.d.	n.d.	10.41	23.05	8.43
8U-10, auger hole in dune swale near VP-1, Virginia Park site										
A/Bw	0–22	5YR6/5	5YR4/6	2f-m sbk	so	0	0, e	1.17	33.17	8.08
Bw[†]	22–47	5YR6/4	5YR5/6	1f-m sbk	lo-so	0	0, es	4.68	31.83	9.18
Btb1	47–58	5YR7/6	5YR6/6	1f-m sbk	so-sh	0	I, ev	4.19	35.25	9.12
Btkb1[†]	58–74	5YR7/4	5YR4/6	2f-m sbk	sh-h	0	II, ev	6.42	38.84	9.56
Bk1b1[†]	74–99	5YR7/3	5YR6/5	3m sbk, 1pl	h-vh	0	II+, ev	11.26	37.18	9.53
Bk2b1[†]	99–154	5YR7/4–7/5	5YR6/5–6/6	2m sbk	h-vh	0	II, ev	11.54	28.74	8.47
Btkqb2[†]	154–220	5YR7/4–7/5	5YR5/7	2m abk	h-vh	0	I, e-es; silica	5.95	27.65	8.09
Bkb2[†]	220–284	5YR7/4–8/4	5YR6/6	n.d.	h-so	0	I, e-es; silica	7.72	14.63	5.06

Note: n.d.—no data.

[†]Value represents average or range of properties of two to five samples within given depth range (see Table DR2).

[‡]Horizon nomenclature and carbonate stage follow Birkeland (1999) and references therein.

[§]Structure codes: Strength/abundance: 1–3. Size: f—fine; m—medium; c—coarse. Shape: sbk—subangular blocky; abk—angular blocky; pl—platy.

[#]Dry consistence codes: lo—loose; so—soft; sh—slightly hard; h—hard; vh—very hard.

[††]Clay film codes: Abundance: 1–3. Thickness: n—thin. Location: br—grain bridge; po—pore filling; pf—ped face.

[‡‡]Carbonate codes: e—effervesces weakly; es—effervesces strongly; ev—effervesces violently.

tional (pipette-sieve) methods for our samples, which are dominantly quartz sands with small amounts of mica and clay-sized particles (Buurman et al., 1997; Hayton et al., 2001). Carbonate was removed with a 15% hydrochloric acid solution, and organic matter was removed with a 30% solution of hydrogen peroxide where needed. Carbonate content was measured with a Chittick apparatus as modified by Machette (1986). Tests on selected samples as well as results from a previous study (Reynolds et al., 2001) showed that organic matter content is typically less than 1% and soluble salt content less than 0.25%; thus, we did not systematically measure these components. Representative data are in Table 2; see Tables DR1 and DR2 for complete data set.[1]

Eolian dust preserved in pothole sediments and surface soils of the Canyonlands area contains silt-sized magnetic particles (Reynolds et al., 2001). We used a combination of magnetic (Thompson and Oldfield, 1986; King and Channel, 1991) and reflected-light petrographic methods to determine the types, amounts, and origins of magnetic minerals. Magnetic property measurements, performed on dried bulk sediment packed into 3.2-cm^3 plastic cubes and normalized for sample mass, included: (a) isothermal remanent magnetization (IRM) acquired at 0.3 Tesla (T), a measure primarily of magnetite; and (b) frequency-dependent magnetic susceptibility (from magnetic susceptibility measurements at 600 Hz and 6000 Hz), a measure of the amount of superparamagnetic (ultrafine, <30 nm) magnetite that may form in some settings by pedogenesis. Contents of Fe and Ti were determined by inductively coupled plasma–atomic emission mass spectroscopy (ICP-AES and ICP-MS) analyses. Table DR3 provides magnetic and Fe-Ti data (see footnote 1).

[1]GSA Data Repository item 2005106, Tables DR1 and DR2 contain particle size and carbonate contents of soils and sediments; Table DR3 contains magnetic and Fe-Ti data; Table DR4 contains pollen data for site VP-2; Fig. DR1 contains probability density plots for OSL data; is available on the Web at http://www.geosociety.org/pubs/ft2005.htm. Requests may also be sent to editing@geosociety.org.

TABLE 3. ^{14}C AGES FROM VIRGINIA PARK AND SALT CREEK

Field sample no.	Lab sample no.*	Material dated	Stratigraphic unit	Depth below surface (m)	^{14}C age†	Calibrated age‡
8U-14 (75 cm)	WW3004	Charcoal in pebbly lens	Base of alluvial fill inset into older dune sand	0.75	4580 ± 50	5250 ± 200
SC-15A	WW3565	Charcoal in burn layer	55 cm below top of alluvial fill; buried by eolian sand	1.55	1900 ± 40	1820 ± 100
SC-15B	WW3566	Charcoal	75 cm below top of alluvial fill; buried by eolian sand	1.75	1840 ± 40	1780 ± 90

*Samples processed at ^{14}C laboratory of the U.S. Geological Survey in Reston, Virginia; analyses performed at NSF-University of Arizona AMS laboratory, Tucson, Arizona.
†Ages expressed as radiocarbon years before A.D. 1950; 1σ error.
‡Calibration performed by the CALIB program (http://radiocarbon.pa.qub.ac.uk/calib/; Stuiver et al., 2003); 2σ error.

Sediment Dating

To determine ages of eolian sands and alluvial deposits, we used optically stimulated luminescence (OSL) dating and ^{14}C analysis of charcoal. For OSL dating, samples were taken from outcrops and pits with PVC pipe hammered horizontally into freshly cleaned faces. Charcoal within the alluvial deposits at the Virginia Park and Salt Creek sites was sampled into plastic bags with metal trowels and analyzed by accelerator mass spectrometry (AMS; Table 3). All radiocarbon ages younger than ca. 20 ka from this and previously published studies were converted to calendar years (cal ka) by the CALIB program of Stuiver et al. (2003).

OSL dating examines the time-dependent signal from the exposure of naturally occurring minerals, typically quartz and feldspar, to ionizing radiation. The technique relies upon the principle that any preexisting luminescence signal contained in the sediment grains is lost on exposure to sunlight during transport. Once the sediment is deposited and shielded from light exposure by the deposition of further sediment, the luminescence signal reaccumulates over time with exposure to radiation from the decay of naturally occurring radioisotopes of uranium, thorium, and potassium and to cosmic radiation. The OSL signal observed in the laboratory is proportional to the time elapsed since the mineral grains were last exposed to sunlight. The OSL age is determined by calibrating the intensity of the OSL signal to a laboratory-administered radiation dose (termed the equivalent dose, D_e) and dividing this value by the annual radiation dose to which the sample was exposed (termed the dose rate). Aitken (1998) provides further details on OSL methods.

For the paleosols formed on dune sand, which typically contain a large component of fine to medium sand from the parent material as well as a lesser component of fines hypothesized to represent dust infiltrated during pedogenesis, we applied OSL techniques to both the medium sand fraction and the fine silt fraction. From the sand fraction, coarse-grained quartz of 90–125-μm diameter was separated with sodium polytungstate, then etched in 40% hydrofluoric acid (HF) for 45 min. From the silt fraction, fine-grained quartz of 4–11-μm diameter was isolated by Stoke's Law settling in sodium oxalate, followed by etching with fluorosilicic acid (H_2SiF_6) for 7 days. For samples 02U-1A-E, 02U-3A, and 02U-3C (Table 4), OSL measurements were conducted solely on the coarse-grained quartz fraction.

Laboratory OSL measurements were performed by an automated Risø[2] TL/OSL reader, equipped with blue LEDs (470 nm) providing ~17 mW cm^{-2} power density and a beta source for irradiations. Three 3-mm Hoya U-340 filters were used to detect the OSL signal. To determine the equivalent dose (D_e) of each sample, a minimum of 24 aliquots was examined for a range of preheat temperatures between 160 and 300 °C by the single-aliquot regenerative-dose measurement procedure of Murray and Wintle (2000), which corrects for changes in the luminescence sensitivity. All OSL measurements were made at 125 ºC. Each aliquot yields an independent estimate of D_e; the mean D_e of between 13 and 23 aliquots was used to determine each 90–125-μm coarse-grained OSL age, and the 4–11 μm fine-grained OSL ages were calculated by using the mean D_e of between 19 and 22 aliquots (Table 4). The uncertainty on D_e was calculated as the standard error of the mean for all samples. Probability density plots for all sample analyses are given in Figure DR1 (see footnote 1).

Pollen Analysis

Pollen analyses were conducted on samples from soil pits in Virginia Park and sediment from trenches at Hamburger Rock. Six samples from sandy, inorganic soil horizons in soil pit VP-2, from a dune swale in Virginia Park (Fig. 2), contained abundant pollen and required no special extraction techniques. Samples were treated with HCl to remove calcium carbonate, screened through a 150-μm sieve, and treated with HF to remove silicates and with HNO_3 and KOH to remove extraneous organic material. Samples were then mounted in glycerin.

Samples collected from Hamburger Rock trenches had low pollen concentrations and required special processing (Cummings, 1999). After treatment with HCl and screening, dispersant was added, and after settling for two hours, clay was removed by pouring off the liquid and suspended clay particles. Organic material was separated from the inorganic fraction in sodium polytungstate, after which HF was used to remove any remaining silicates.

A minimum of 200 pollen grains from each sample was identified at 400×–600× magnification; a few were examined in more detail at 1000×. Grains that were distorted or degraded beyond recognition were noted and included in total pollen counts. Grain aggregates, indicating proximity of a plant to the study site, were counted as single grains. Complete data are in Table DR4 for VP-2 and in Cummings (1999) for Hamburger Rock (see footnote 1).

STRATIGRAPHY, PEDOLOGY, AND AGES OF DEPOSITS

In this section, we discuss the character of the stratigraphic units and paleosols exposed at each of the five study sites, ages of the deposits, and correlations among multiple exposures, pits, and auger holes at individual study sites. We also use magnetic and chemical data for paleosols formed on eolian sand in Virginia Park to infer the duration and nature of pedogenesis, including additions of far-traveled eolian dust to the soils.

Eolian Deposits and Soils, Virginia Park

Auger holes, pits, and outcrops in the Virginia Park area (Table 1; Fig. 2) exposed sequences of eolian sand separated by poorly to moderately

[2]Use of trade names is for descriptive purposes only and does not imply endorsement by the U.S. Geological Survey.

TABLE 4. EQUIVALENT DOSE (D_e), DOSE RATES, AND OPTICALLY STIMULATED LUMINESCENCE (OSL) AGES

Sample no.*	Depth (m)	Stratigraphic unit	Grain size analyzed (μm)	D_e (Gy)†	n‡	U (ppm)§	Th (ppm)§	K (%)§	Infinite α dose rate#	Infinite β dose rate#	External α dose rate "wet"##	External β dose rate "wet"##	External γ dose rate "wet"##	Cosmic#	Total dose rate#	Age (10^3 yr)**
							VP-1, soil pit in dune crest, Virginia Park site										
OSL-1	0.40	Surface soil, B2tk horizon	90–125	26.6 ± 0.6	20	2.22 ± 0.25	6.34 ± 0.82	2.04 ± 0.07	—	2.10	—	1.83	1.00	0.274	3.10 ± 0.08	8.6 ± 0.3
OSL-1	0.40	Surface soil, B2tk horizon	4–11	28.1 ± 0.5	22	2.22 ± 0.25	6.34 ± 0.82	2.04 ± 0.07	10.8	2.10	0.377	1.98	1.00	0.274	3.63 ± 0.13	7.7 ± 0.3
OSL-2	0.65	Paleosol, B32tkb horizon	90–125	40.1 ± 0.8	22	2.34 ± 0.21	4.54 ± 0.67	1.98 ± 0.06	—	2.01	—	1.75	0.92	0.248	3.07 ± 0.07	13.8 ± 0.4
OSL-2	0.65	Paleosol, B32tkb horizon	4–11	43.7 ± 0.9	20	2.34 ± 0.21	4.54 ± 0.67	1.98 ± 0.06	9.8	2.01	0.343	1.90	0.92	0.248	3.40 ± 0.12	12.8 ± 0.5
							VP-2, soil pit in dune swale, Virginia Park study site									
OSL-3	0.40	Surface soil in reworked(?) eolian sand, Bwk horizon	90–125	11.4 ± 0.4	23	2.22 ± 0.22	4.97 ± 0.70	1.72 ± 0.06	—	1.81	—	1.58	0.87	0.274	2.72 ± 0.07	4.2 ± 0.2
OSL-3	0.40	Surface soil in reworked(?) eolian sand, Bwk horizon	4–11	12.0 ± 0.3	19	2.22 ± 0.22	4.97 ± 0.70	1.72 ± 0.06	9.8	1.81	0.343	1.71	0.87	0.274	3.19 ± 0.12	3.8 ± 0.2
OSL-4	0.80	Paleosol in reworked(?) eolian sand, Btk2b horizon	90–125	21.7 ± 0.4	20	1.77 ± 0.25	6.88 ± 0.82	1.84 ± 0.06	—	1.84	—	1.64	0.93	0.239	2.81 ± 0.07	7.7 ± 0.2
OSL-4	0.80	Paleosol in reworked(?) eolian sand, Btk2b horizon	4–11	22.5 ± 0.6	22	1.77 ± 0.25	6.88 ± 0.82	1.84 ± 0.06	10.0	1.84	0.348	1.78	0.93	0.239	3.30 ± 0.12	6.8 ± 0.3
							8U-14, arroyo cut, Virginia Park site									
OSL-5††	0.73	Alluvial pebbly sand	90–125	~18–31††	16	1.32 ± 0.12	2.62 ± 0.36	1.40 ± 0.03	—	1.36	—	1.18	0.59	0.242	2.01 ± 0.05	~9–16††
OSL-5††	0.73	Alluvial pebbly sand	4–11	~13–23††	20	1.32 ± 0.12	2.62 ± 0.36	1.40 ± 0.03	5.6	1.36	0.195	1.28	0.59	0.242	2.30 ± 0.07	~6–10††
OSL-6	1.54	Paleosol in eolian sand	90–125	75.3 ± 1.3	16	1.14 ± 0.08	1.60 ± 0.26	1.14 ± 0.03	—	1.10	—	0.96	0.46	0.216	1.63 ± 0.04	46.1 ± 1.4
OSL-6	1.54	Paleosol in eolian sand	4–11	74.5 ± 1.3	21	1.14 ± 0.08	1.60 ± 0.26	1.14 ± 0.03	4.3	1.10	0.152	1.04	0.46	0.216	1.87 ± 0.06	40.0 ± 1.4
							9U-21, arroyo cut, graben-fill site									
02U-3C	1.70	Unit 2 in graben-fill deposits, 2Ckb1 horizon	90–125	41.9 ± 0.7	17	2.54 ± 0.21	5.64 ± 0.67	1.59 ± 0.05	—	1.77	—	1.54	0.90	0.216	2.66 ± 0.08	15.8 ± 0.6
02U-3B†	2.80	Unit 3 in graben-fill deposits, 3Cb2 horizon	90–125	43.9 ± 0.8	16	0.99 ± 0.09	2.20 ± 0.30	1.18 ± 0.03	—	1.13	—	0.95	0.47	0.183	1.60 ± 0.05	27.4 ± 1.0
02U-3B†	2.80	Unit 3 in graben-fill deposits, 3Cb2 horizon	4–11	52.6 ± 1.0	20	0.99 ± 0.09	2.20 ± 0.30	1.18 ± 0.03	4.4	1.13	0.146	1.03	0.47	0.183	1.83 ± 0.06	28.8 ± 1.1
02U-3A	6.10	Unit 4 in graben-fill deposits, 3Cb3 horizon	90–125	74.2 ± 1.1	16	1.39 ± 0.20	5.58 ± 0.64	1.24 ± 0.05	—	1.32	—	1.11	0.67	0.131	1.91 ± 0.06	38.8 ± 1.4
							ISKY dune, sand pit north of Canyonlands National Park									
02U-1E	0.47	Unit 1, eolian sand	90–125	1.8 ± 0.1	13	1.38 ± 0.10	1.94 ± 0.31	1.27 ± 0.03	—	1.25	—	1.05	0.52	0.275	1.84 ± 0.05	1.0 ± 0.04
02U-1D	2.30	Unit 2, eolian sand	90–125	3.7 ± 0.1	17	1.24 ± 0.11	2.56 ± 0.35	1.52 ± 0.04	—	1.44	—	1.26	0.60	0.204	2.06 ± 0.06	1.8 ± 0.1
02U-1C	5.60	Unit 3, eolian sand	90–125	31.0 ± 0.7	14	2.25 ± 0.16	3.40 ± 0.51	1.80 ± 0.05	—	1.83	—	1.59	0.82	0.140	2.55 ± 0.08	12.2 ± 0.5
02U-1B	6.75	Unit 4, eolian sand	90–125	32.7 ± 0.5	15	1.57 ± 0.12	2.35 ± 0.36	1.49 ± 0.03	—	1.46	—	1.27	0.62	0.124	2.01 ± 0.06	16.2 ± 0.5
02U-1A	8.85	Unit 5, eolian sand	90–125	40.4 ± 0.9	16	2.13 ± 0.19	4.92 ± 0.60	1.55 ± 0.06	—	1.66	—	1.45	0.82	0.101	2.36 ± 0.07	17.1 ± 0.7

*Corresponding Aberystwyth Luminescence Laboratory sample codes are as follows: OSL-1 = *Aber/59CY1*; OSL-2 = *Aber/59CY2*; OSL-3 = *Aber/59CY3*; OSL-4 = *Aber/59CY4*; OSL-5 = *Aber/59CY5*; OSL-6 = *Aber/59CY6*; 02U-3C = *Aber/71CY3C*; 02U-3B = *Aber/59CY7*; 02U-3A = *Aber/71CY3A*; 02U-1E = *Aber/71CY1E*; 02U-1D = *Aber/71CY1D*; 02U-1C = *Aber/71CY1C*; 02U-1B = *Aber/71CY1B*; 02U-1A = *Aber/71CY1A*.

†Probability density plots showing individual D_e determinations are shown in Figure DR4.

‡n is the number of D_e determinations.

§Concentrations of U, Th, and K were calculated from laboratory-based thick source alpha counting (TSAC) and beta counting measurements of dried, powdered, bulk material, and are shown to three significant figures.

#Dose-rate values (Gy/10^3 yr) have been rounded to three significant figures, but the total dose rates and ages have been calculated by values before rounding. Dose rates were calculated using an α-value of 0.040 ± 0.002 (Rees-Jones, 1995) where appropriate, and assuming a water content (assessed in the laboratory using sealed field samples, and expressed as percentage dry mass) of 4 ± 2% for samples OSL-1 to -6, 7 ± 3% for samples OSL-7 and 02U-3A and -1E, and 4 ± 3% for samples 02U-3C and -1A to -1D. The cosmic-ray dose rate was calculated for each sample on the basis of the depth, altitude, and geomagnetic latitude (Prescott and Hutton, 1994). Central values are given for dose rates; errors are incorporated into that given for the total dose rate.

**Luminescence ages are expressed as thousands of years before A.D. 2000 and calculated to one decimal place.

††Sample OSL-5 shows scatter in the D_e distribution, believed to be the result of incomplete bleaching on deposition. For this sample, D_e ranges and age ranges are therefore presented in the table, all of which may overestimate the true depositional age. See discussion in the text and probability density plots (Fig. DR1).

developed silt- and $CaCO_3$-enriched soils that formed in the sand layers (Table 2 and Fig. 5). Each soil probably reflects at least a few thousand years of surface stability, during which erosion modified the dune surfaces in a setting similar to that of the present day. However, the morphology, texture, and composition of the surface soils are different from properties of many of the buried soils.

Soil pits in a dune crest (VP-1) and a swale (VP-2) provide detailed information on the near-surface soils and sediments. Data from these pits and the auger holes (Table 2; Fig. 5) suggest that the upper 40–50 cm represent a weakly developed (A/Bw horizon sequence) modern soil forming in eolian sand that overlies a better-developed soil (silty, sometimes clay enriched, Bt or Btk horizon). The boundary between these two soils is not obvious visually, but it is clearly indicated by a sharp increase downward in both silt and clay content and magnetite content (Fig. 5). These relations suggest that a former stable land surface on which the Bt/Btk horizon developed has been buried by a thin sand layer in which the modern soil is forming; pedogenic processes have partially blended or "welded" the two soils.

At depths of ~1.3–1.8 m, each auger hole penetrated the top of a second buried soil (Figs. 5 and 6). These paleosols appear less well developed than the upper buried soils; the deeper paleosols typically are thinner and less enriched in silt and carbonate, have lower IRM values, and display little or no evidence of translocated clay (Fig. 5, Table 2). Their consistent depth in auger holes throughout the study site (Fig. 6) suggests they represent an older episode of surface stability and soil formation that was interrupted by deposition of the overlying eolian sand. On the basis of paleosol properties, this older episode of stability was probably shorter or less conducive to weathering and translocation of fines than the younger episode. At depths of ~2.8–3.0 m, at least two of the auger holes penetrated a third buried soil (Fig. 6), suggesting a third episode of stability and pedogenesis. These paleosols also appear to be weakly developed; they show little increase in silt, clay, or IRM value (Tables DR2 and DR3 [see footnote 1]), but they do exhibit an increase in pedogenic $CaCO_3$.

The soil-paleosol complex at the surface, although ubiquitous in the study site, is expressed differently at different topographic positions. In dune-crest positions, such as auger hole 8U-11 and pit VP-1 (Figs. 5 and 6, Table 2), the soils and sediments contain less silt and $CaCO_3$ than in dune-swale positions (8U-10 and VP-2). Clay is present in similar amounts but is concentrated in the upper parts of Bt horizons in crest soils and is more uniformly distributed with depth in the

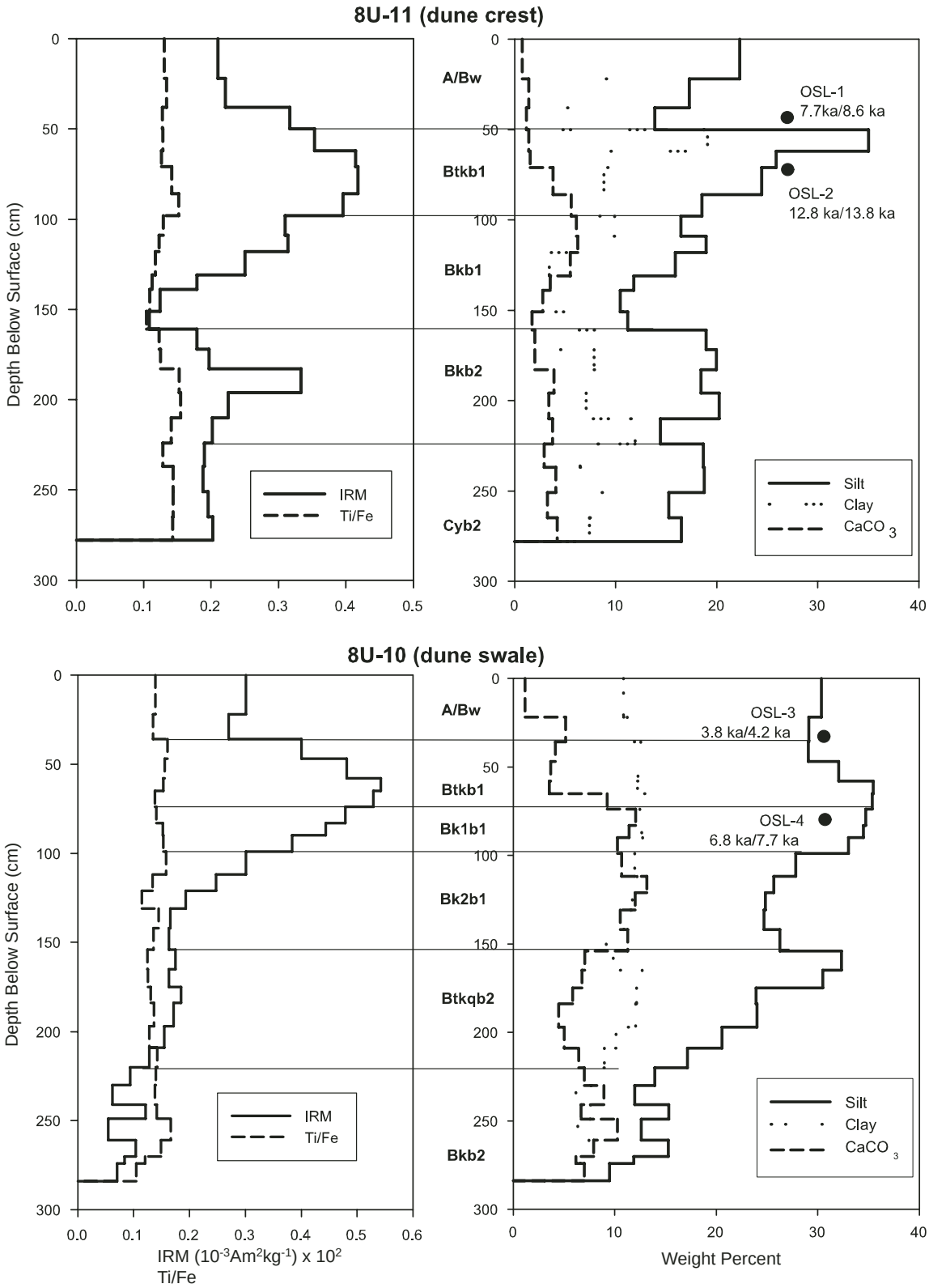

Figure 5. Examples of depth trends in particle size, $CaCO_3$, and magnetic properties in auger holes at the Virginia Park site (locations in Fig. 2; see Tables DR1, DR2, and DR3 for complete data [see footnote 1]). Silt and clay in weight percent of carbonate-free <2 mm fraction; $CaCO_3$ in percent of total sample. Horizontal lines are boundaries between soil horizons (Btkb1, etc.; lowercase "b" designates buried soil, numbered sequentially downward). Upper part of 8U-11, to depth of 1 m, examined in more detail in nearby soil pit VP-1; upper part of 8U-10, to depth of 1.2 m, examined in soil pit VP-2. Dots show depths and ages of optically stimulated luminescence (OSL) samples (Table 4) from soil pits. IRM—isothermal remanent magnetization.

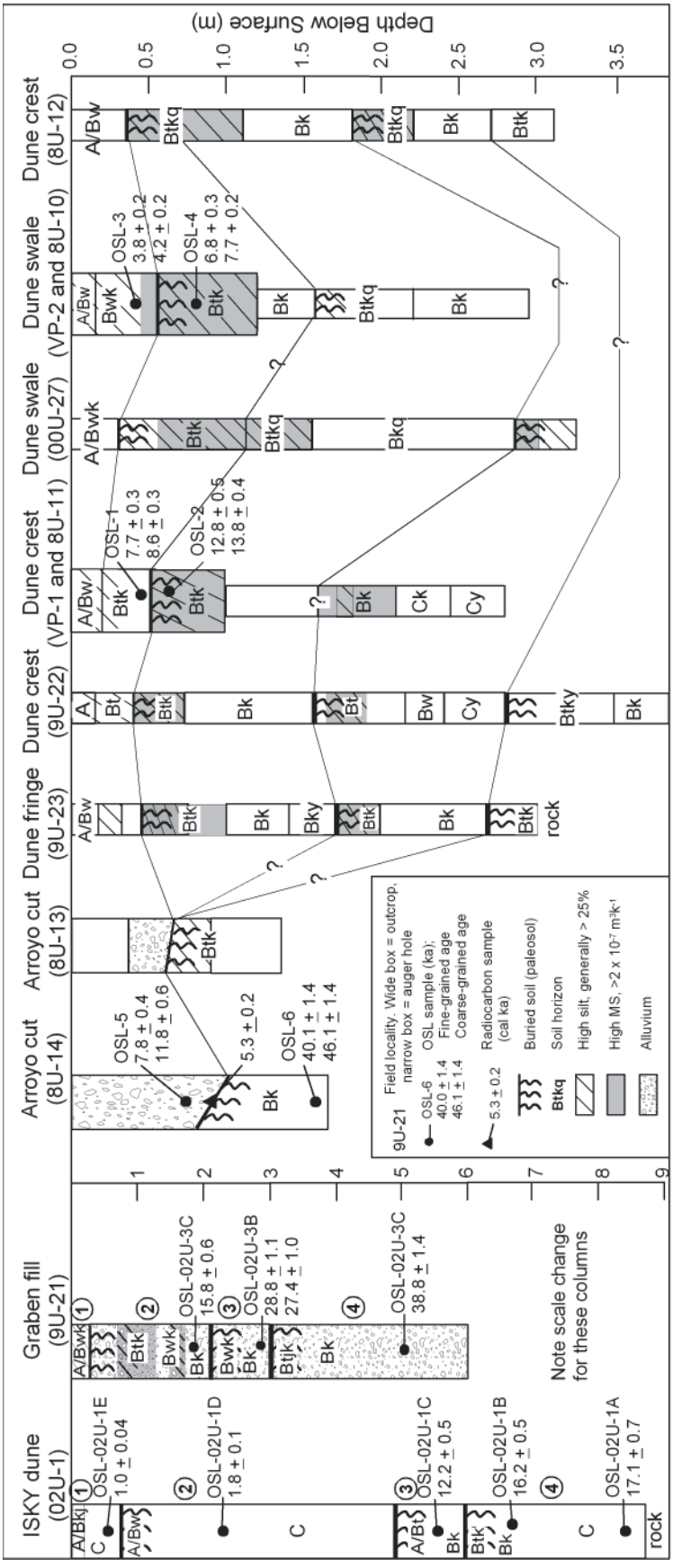

Figure 6. Correlations and ages of eolian and alluvial units and paleosols at ISKY dune, Virginia Park, and graben-fill site (locations in Figs. 1 and 2). Letters (A, Bk, Bt, etc.) indicate general designation of soil horizon (see Tables DR1, DR2, and DR3 for soil data; no soil samples collected from ISKY site [see footnote 1]). Circled numbers are depositional units recognized at outcrop sites 02U-1 and 9U-21 (Fig. 3). Dots with two optically stimulated luminescence (OSL) ages (Table 4) reflect presumed depositional age of coarse-grained (90–125 μm diameter) quartz (lower number) and infiltration age of fine-grained (4–11 μm diameter) quartz (upper number). Only coarse-grained quartz measured at dots with one OSL age. Ages for OSL-5 at site 8U-14 interpreted as overestimates (see text).

swales. These differences may reflect transport and concentration of fines from the topographically higher dune crests into adjacent swales by wind eddying and sheetwash, as well as more efficient trapping of fines by denser vegetation in the swales. In addition, accumulation of $CaCO_3$ is enhanced in swales.

Magnetite content of the soil and sediment samples increases at or near the tops of the paleosols, and corresponds closely with silt content (Fig. 5). IRM values of sediment (0.55–5.4 $\times 10^{-3}$ Am^2 kg^{-1}) are much greater than values of the local bedrock of the Virginia Park study site, the Cedar Mesa Sandstone (typically 0.05–0.1 $\times 10^{-3}$ Am^2 kg^{-1}; Reynolds et al., 2001), the source of most of the eolian sand in the dune field. Strongly magnetic minerals in the soils consist of silt-size (typically 4–20 μm) magnetite and titanomagnetite, commonly intergrown with minerals such as hematite, ilmenite, and ilmenorutile, typical of formation in igneous rocks (Haggerty, 1976). These strongly magnetic minerals are absent in the local bedrock of the study area; thus, residual concentration and subsequent eolian erosion of magnetic minerals from local rocks cannot account for the magnetic and petrographic results.

Complementary magnetic and petrographic results indicate that the variations in IRM are primarily related to varying inputs of detrital magnetite and not to pedogenic growth of magnetic grains or postdepositional destruction of detrital magnetite. (1) IRM and magnetic susceptibility are strongly correlated (r^2 is 0.99 and 0.98 for 8U-10 and -11, respectively), indicating no magnetic enhancement by ultrafine-grained pedogenic iron oxides that are too small to carry IRM. (2) Values of frequency-dependent magnetic susceptibility, which measures ultrafine, possibly pedogenic magnetite, are low, and their minor variations do not correspond to the high magnetic mineral content associated with the paleosols (Table DR3 [see footnote 1]). (3) Chemical data show no indication of postdepositional iron mobility: the content of chemically immobile Ti generally tracks IRM, and Ti/Fe values vary little (Fig. 5). (4) Petrographic observation of magnetite particles shows no indication of pedogenic alteration of detrital magnetite.

Because silt-sized magnetite and titanomagnetite are abundant in the surface and buried soils but absent in nearby sedimentary rocks, their presence is best explained by windborne dust. Preliminary comparisons of magnetic properties, particle size, and elemental contents of soils, modern dust, and local bedrock suggest that surficial sediment (0–10 cm depth) in the study area may contain as much as 20% dust derived from source terrains of igneous rocks (Reynolds et al., 2001, 2003). Silt and IRM

covary even in the deeper paleosols despite their generally lower contents compared with near-surface soils, indicating that infiltration of magnetic, far-traveled dust also occurred in the past but had less importance.

Both the coarse-grained and fine-grained aliquots of the OSL samples examined gave rise to single-population D_e (equivalent dose) distributions (e.g., Figs. DR1A, B [see footnote 1]), with the exception of one sample (OSL-5), which demonstrated scattered D_e distributions (Figs. DR1I, J [see footnote 1]). Sample OSL-5 was taken from an alluvial pebbly sand layer and is mainly composed of dune sand with an alluvial transport distance of <0.5 km, likely reworked from eolian deposits of different ages (Fig. 2). Thus, the sediment may not have been exposed to sufficient light during transport downstream to fully reset, or "bleach," the preexisting luminescence signal before deposition. Such "incomplete bleaching" makes it difficult to identify the true depositional age of the sediments. Although the approach could be taken that the smallest D_e determinations for sample OSL-5 are likely to be the most appropriate, in reality, it is highly likely that all of these D_e values will yield age overestimates (Figs. DR1I, J [see footnote 1]). The presence of incompletely bleached grains in OSL-5 is supported by the fact that both coarse-grained and fine-grained OSL ages (Table 4) are significantly older than a radiocarbon age of 4.58 ± 0.05 ka (5.3 ± 0.2 cal ka) from charcoal at the base of the same unit (Table 3). On the basis of the smallest D_e determinations alone, the OSL ages calculated are still older than the radiocarbon age, being ca. 8.99 ka and 5.76 ka for coarse grains and fine grains, respectively. The OSL age ranges given for sample OSL-5 in Table 4 should therefore be regarded as age overestimates and are not discussed further in this paper.

The uncertainties on the OSL age determinations are small, ≤5% for all samples except OSL-5 (Table 4). All OSL ages are in stratigraphic order within 1σ uncertainties (Figs. 3A, B, and 6). The coarse-grained and fine-grained quartz OSL ages (OSL-1, -2, -3, -4, -6) are indistinguishable at 1σ error for samples OSL-2 and 02U-3B, and at 2σ error for samples OSL-1 and OSL-4; thus, the ages of the two fractions are statistically the same. However, except for sample 02U-3B, the mean ages determined for all fine-grained OSL analyses are younger than those of respective coarse-grained OSL analyses. The slightly younger fine-grained ages may result from younger silt infiltrating the dune sands during pedogenesis.

The coarse-grained quartz OSL ages of the eolian sand units in the dune-crest and -swale sites and the buried sand unit in the arroyo cut indicate three or four episodes of eolian activity during the late Quaternary (Table 4, Fig. 6). Coarse-grained OSL ages of 8.6 ± 0.3 ka and 4.2 ± 0.2 ka were determined for the uppermost thin sand (samples OSL-1 and -3), and ages of 13.8 ± 0.4 ka and 7.7 ± 0.2 ka for the first buried sand (samples OSL-2 and -4). The older ages for the two units were obtained on samples from the dune-crest pit (site VP-1), whereas the younger ages were from the dune-swale pit (site VP-2). The differing ages have three possible explanations: (1) they represent long spans of time (4000–5000 yr) when the dunes were active; (2) the younger ages in the swale site reflect a reactivation of eolian sedimentation in the late Holocene that was not recorded at the crest site; and (3) the younger ages in the swale site reflect sheetwash reworking of sediment derived from the dune crests. The similarity between the younger OSL age on the crest, 8.6 ± 0.3 ka, and the older OSL age in the swale, 7.7 ± 0.2 ka, suggests that these units are correlative (the ages overlap at 2σ analytical uncertainty) and that 2 above is the likely explanation (possibly modified by sheetwash redistribution). An OSL age of ca. 46 ka (sample OSL-6), obtained on a truncated dune sand exposed in an arroyo cut (site 8U-14), indicates an earlier period of eolian activity. Charcoal at the base of the alluvium overlying this old dune sand gave a ^{14}C age of ca. 5.3 cal ka (Table 3, Fig. 6).

We correlate the sand units and paleosols in the Virginia Park site by using pedogenic and magnetic properties of the paleosols and the OSL ages (Fig. 6). Because of the uncertainty in extrapolating between auger holes, the ages and correlation of units beneath the surface soil-paleosol couplet are speculative. The top of the arroyo cut that exposes ca. 46 ka eolian sand is at least 3 m lower in altitude than the dune crests (Fig. 2); thus, this oldest paleosol and sand unit probably correlates to one of the two deeper paleosols in the auger holes. The concentrations of silt and clay in the less truncated paleosol at arroyo site 8U-13 are closer to those preserved in the paleosols at ~2 m depth in nearby auger holes. Paleosols in the swale holes may have been overthickened by sheetwash accretion during pedogenesis and are commonly welded, adding to the difficulty in correlating to the crest auger holes. Assuming that the units represented by samples OSL-1 and OSL-4 are in fact the same age, ca. 7.7–8.6 ka, then the most likely correlations of deeper units suggest that the crests and swales are relatively long-lived features in which equivalent units appear at shallower depths in crest positions than in swale positions (Fig. 6).

Stratigraphy and Ages at ISKY Dune

Four eolian sand units are exposed in the sand pit at the ISKY dune (Figs. 3A and 6), each capped by a soil. The youngest unit is only ~0.7 m thick, and the OSL age is 1.0 ± 0.04 ka (Table 4, sample 02U-1E), consistent with the morphology of the surface soil, which is characterized by a slightly darkened A horizon and traces of secondary $CaCO_3$. Unit 2 is ~4.2 m thick, much thicker than the other units here and at Virginia Park; a sample from 1.6 m below the base of unit 1 gave an OSL age of 1.8 ± 0.1 ka (sample 02U-1D). The paleosol capping unit 2 is characterized by a weak Bw horizon, with only slight reddening and traces of secondary $CaCO_3$, consistent with a surface exposure of several hundred years.

The outcrop is divided vertically by a prominent bench developed on the relatively resistant paleosol formed in unit 3, which has an OSL age of 12.2 ± 0.5 ka (sample 02U-1C; Fig. 3A and Table 4). This paleosol is characterized by an A-Bt-Bk horizon sequence with stage 2 $CaCO_3$ near the base, where the Bk is partly superimposed on a paleosol formed on unit 4. The moderate development of this paleosol is consistent with a longer exposure time than those formed on the younger units and is similar in character to the paleosol formed in the eolian sand of similar age (13.8 ka) at Virginia Park (sample OSL-2). However, the paleosol in Virginia Park apparently formed in only ~5000 yr, rather than the ~10,000 yr suggested by the difference in the ages of units 2 and 3 at the ISKY site. We do not know whether this apparently lengthy hiatus is real, or whether an intervening early to middle Holocene eolian unit was deposited and later eroded or was not recognized during sampling.

Unit 4, which is 2.8 m thick, is characterized by a weaker soil than unit 3, including a possible Bw or Bt horizon welded to the overlying Bk of unit 3. Unit 4 aggraded relatively quickly at ca. 17–16 ka; the two OSL ages, although in correct stratigraphic order, overlap within 1σ analytical error (samples 02U-1B and -1C, Table 4 and Fig. 3A). The soil formed in unit 4 is consistent with an exposure age of a few thousand years.

Stratigraphy and Soils at Hamburger Rock

Several trenches excavated northwest of Hamburger Rock exposed soils formed in thin eolian sands overlying weathered red siltstone and shale; one, trench 7, exposed a thick deposit of sheetwash alluvium on the south side of the hill (Figs. 1 and 7). No radiometric ages were obtained, but soil properties and pollen data (discussed below) allow relative age assessment. The following discussion is modified from the Shearin et al. (2000) report on the site excavation and analyses.

Unit 1 represents very recent deposition of eolian sand in the area around Hamburger Rock. This sand blankets much of the area, including

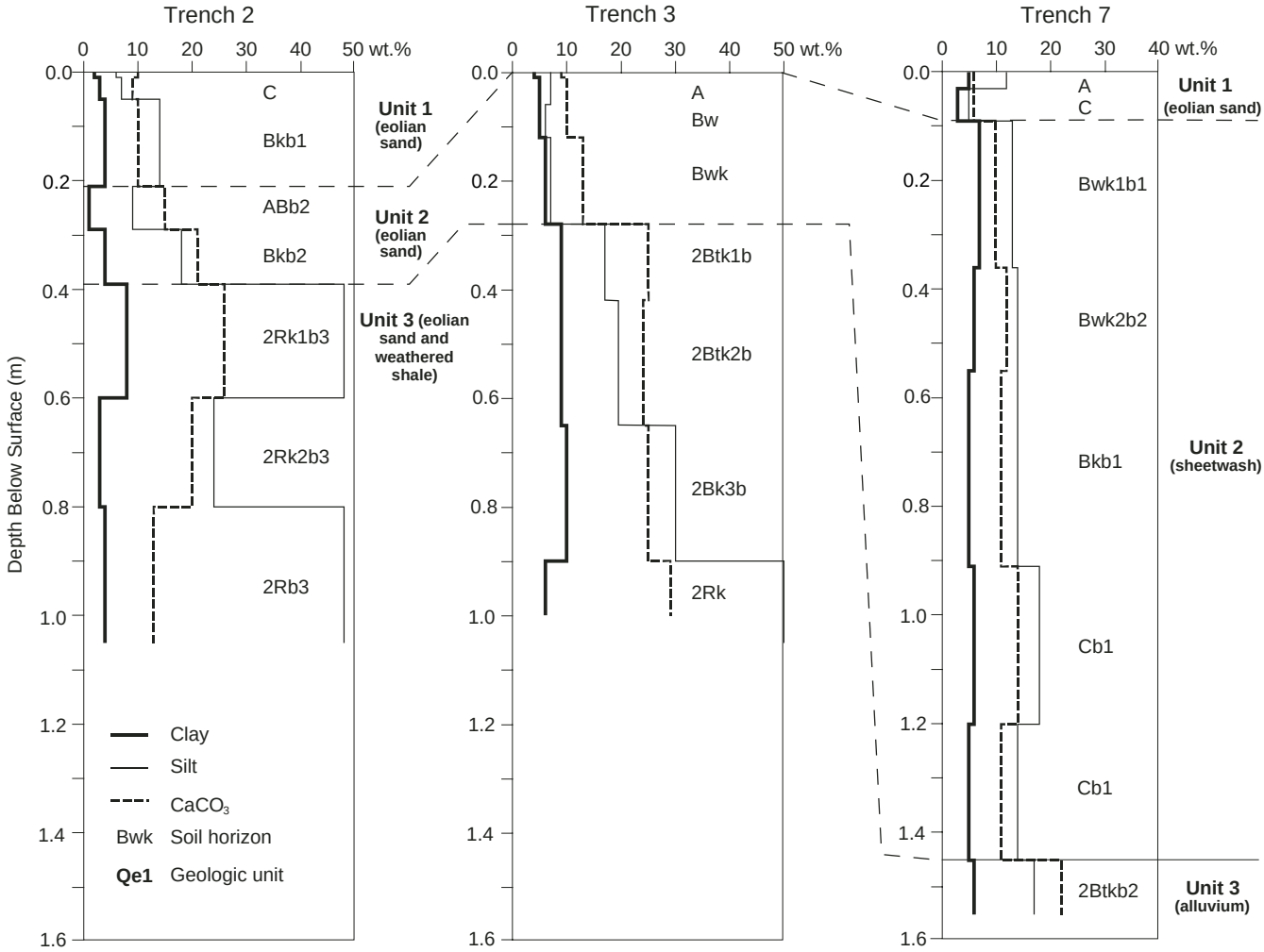

Figure 7. Depth trends in particle size and $CaCO_3$ in trenches (no analyses performed on samples from trench 5) at Hamburger Rock site (location in Fig. 1). Dashed lines indicate correlations based on soil properties.

the upper part of the sheetwash deposits exposed in trench 7. Two episodes of sand deposition are indicated by the weak buried soil (Bkb1) overlain by fresh sand (C) in the upper 20 cm of trench 2 (Fig. 7). Unit 1 has little pedogenic imprint, only a very slight increase in silt and clay, and small flecks of secondary $CaCO_3$. Such characteristics indicate an age of probably less than 500 yr. A piece of glass at the contact between units 1 and 2 in trench 2 supports an age of less than 150 yr for some of this unit.

Unit 2 in trenches 2, 3 (Fig. 7), and 5 (Shearin et al., 2000) represents an older period of eolian sand transport and deposition followed by pedogenesis before burial by unit 1. This deposit bears a soil with fairly consistent properties, including a brownish (2.5YR 4/6) A horizon and a Bwk horizon with stage 1 $CaCO_3$. The upper contact of this soil is quite irregular where buried by unit 1. In places, this irregularity is imparted by burrows, but in other places, the A and Bwk horizons seem compacted and indented, perhaps by hoofs. The properties of the soil formed on eolian unit 2 are similar to dated soils elsewhere that are middle to late Holocene in age (e.g., unit 1 at Virginia Park and unit 2 at the ISKY site), suggesting that soil formation and surface stability may have lasted one to a few thousand years after deposition of unit 2.

In trench 3, an older paleosol formed on eolian sand mixed with weathered bedrock suggests a yet older episode of sand deposition and soil formation (unit 3, Fig. 7). In trenches 2 and 5, a truncated paleosol formed on bedrock. The older paleosol has much stronger development of pedogenic $CaCO_3$ than do the younger soils and locally has a Bt horizon. However, the abundant silt contained by this paleosol is largely derived from the silty shale. The moderately developed Bk and Bt horizons indicate a significantly longer duration of soil formation than indicated for the overlying younger soils, and may also imply higher effective moisture sufficient to translocate clay particles.

In trench 7, unit 2 represents accumulation of sheetwash in a gently sloping drainageway. The overthickened weak Bw and Bk horizons that compose most of the deposit and the apparent absence of unconformities (Fig. 7) indicate that this sheetwash accumulated gradually over a long period of time, uninterrupted by significant erosion. Unit 2 overlies a paleosol that apparently formed on somewhat coarser alluvium (unit 3, poorly exposed at the pit bottom). This paleosol has a Bt horizon and quantity of pedogenic $CaCO_3$ similar to those of the paleosols formed on unit 3 in trenches 2 and 3.

Stratigraphy and Ages of Graben-Fill Deposits

A deep cut in Chesler Canyon exposes more than 6 m (Figs. 3B and 6; basal ~2 m of the outcrop too deeply buried by colluvium

to examine) of sediment and paleosols that accumulated within a southern extension of the Devils Pocket, the easternmost graben of The Grabens area of Canyonlands National Park. Unit 1 thickens upslope toward the adjacent bedrock; where sampled, it appears to be eolian sand. Units 2, 3, and 4 consist of silt and sand with minor amounts of granule-to-pebble clasts floating in the finer matrix. Unit 2, the thickest, is roughly stratified with local concentrations and lenses of fine pebbles, especially in the basal 1 m, where unit 2 fills a subdued channel cut into unit 3. Units 3 and 4 are slightly more coarsely grained than unit 2 and are more poorly stratified, with fewer pebble lenses. We interpret these three units to consist mainly of colluvium with minor alluvial reworking.

OSL dating provides ages of the deposits in the graben fill. The surface soil formed on undated eolian sand has an A-Bwk horizon sequence with abundant silt (>30%), suggesting a correlation to surface soils in the Virginia Park site (Figs. 5 and 6). A thick, moderately developed paleosol with significant amounts of infiltrated silt and secondary $CaCO_3$ is preserved in the upper 1.5 m of unit 2. This soil is similar to, but thicker than, those formed on 12–13 ka dune sands at the Virginia Park and ISKY sites. OSL sample 02U-3C near the base of unit 2 yielded an age of 15.8 ± 0.6 ka (Table 4), consistent with the degree of paleosol development. Units 3 and 4 both have paleosols with weaker horizonation, primarily Bwk-Bk sequences with stage 1 secondary $CaCO_3$. The coarse-grained OSL age from unit 3 is 27.4 ± 0.9 ka (sample 02U-3B), and the age from unit 4 is 38.8 ± 1.4 ka (sample 02U-3A). Thus, the graben fill deposits represent three separate late Pleistocene episodes of aggradation by colluvial transport and alluvial reworking, each episode followed by several thousand years of pedogenesis, then by minor erosion and more aggradation. Incision of this thick fill by Chesler Wash must have begun after 16 ka and perhaps much later, because more than 1.5 m of sediment with cumulic soil properties (unit 1) accumulated atop the youngest dated layer.

Stratigraphy and Ages of Salt Creek Terraces

Salt Creek, a tributary of the Colorado River (Fig. 1), is bordered by a prominent flight of five terraces (Fig. 4). The upper terrace surface (T5) lies 8.5–10 m above the modern channel and is partly covered by alluvial sediment derived from small tributary drainages. T5 is the oldest major fill terrace observed in the study area and is well preserved in many locations. Texturally, this terrace fill is dominantly sand and interbedded silt and clay, but contains a gravel layer near the base. Radiocarbon analyses on both charcoal and burn layers within the upper one meter of the terrace gave calibrated ages (2σ) of 1815 ± 90 and 1780 ± 90 yr B.P. (Table 3). These ages suggest that aggradation culminated at ~1800 yr B.P., probably just before incision.

Younger terrace surfaces in the study area (T4 through T2) except for the most recent floodplain terrace (T1) are cut terraces formed in T5 fill (Fig. 4). T1 is the modern floodplain and consists of sand and gravel like that in the modern stream channel. We found no dateable material in the younger terraces. Lag gravels capping bedrock represent older Holocene and probably Pleistocene episodes of alluviation, but are poorly preserved and have not been dated (V.S. Williams, U.S. Geological Survey, 2004, personal commun.).

POLLEN DATA, INTERPRETATION, AND SITE CORRELATIONS

The following section presents and interprets pollen data from Virginia Park and Hamburger Rock, and discusses correlation between them. Our interpretation of paleoclimate from the pollen data is founded on correlation of sequences that are based on stratigraphy and paleosol properties. We recognize that these deposits and soils represent records with significant hiatuses, especially the thin eolian deposits and truncated paleosols from trenches 2, 3, and 5 at Hamburger Rock.

Pollen analyses from the Hamburger Rock trenches (Cummings, 1999), coupled with correlations among eolian deposits and paleosols, indicate significant changes in vegetation communities during the Holocene, which in turn imply substantial climate changes. Twelve pollen samples from trench 7 provide a continuous sequence of analyses showing systematic changes in local plant species (Fig. 8). Samples FS15, -17, and -18 from alluvial unit 3 contain relatively abundant grass and arboreal pollen (mainly *Pinus* and *Juniperus* but also some *Picea*, probably from long-distance transport), as well as pollen from grapes (*Vitis*). Cheno-Am-type pollen (Chenopodiaceae-*Amaranthus*), common to abundant in all samples, is a smaller percentage of total pollen in unit 3; small amounts of *Ephedra nevadensis* type (Mormon tea) pollen are also present. Pollen from *Abronia*, low-spine Asteraceae, and *Sphaeralcea* indicates plants adapted to disturbed habitats, such as an active floodplain.

Above the paleosol capping unit 3, from ~110 cm upward to 40 cm depth in sheetwash unit 2, arboreal pollen decreases by half and Cheno-Am pollen doubles (Fig. 8), suggesting an increase in aridity. *Picea* pollen is absent. Pollen indicators of disturbed habitat persist, as might be expected in this drainageway. *Artemisia*, which was found throughout the section, spikes in sample FS13 at ~105 cm. *Ephedra torreyana* appears at the base of unit 2 and maintains a fairly constant presence upsection, whereas *E. nevadensis* increases upward. Martin (1963) has interpreted the relative amounts of these two pollen types as an indicator of seasonality of precipitation: *E. torreyana*–type species prefer areas of summer-dominant precipitation, whereas *E. nevadensis*–type species prefer winter-dominant precipitation. Thus, the appearance of *E. torreyana* may signal somewhat increased summer precipitation during deposition of unit 2.

In the upper 40 cm of trench 7, these pollen trends reverse. Arboreal pollen increases substantially, with *Juniperus* as abundant as *Pinus* for the first time and *Picea* reappearing, whereas Cheno-Am pollen decreases. In the two samples from the top 10 cm, pollen indicators of disturbed habitat such as low-spine Asteraceae increase dramatically, possibly as a response to historic surface disturbance. *Artemisia* pollen decreases sharply. The presence of pollen from *tamarix* (tamarisk, a nonnative species introduced in the 20th century) in unit 1 indicates that these sediments are less than 100 yr old.

The truncated paleosols formed on sand and weathered bedrock in trenches 2, 3, and 5 are provisionally correlated, on the basis of stratigraphy and soil properties, with unit 3 at the base of trench 7 (Fig. 7). Pollen distributions of samples FS5 and FS16-2 and -3 from these paleosols are broadly consistent with this correlation (Fig. 9). Each sample has relatively large amounts of arboreal pollen, small amounts of Cheno-Am pollen, and more *Artemisia* pollen than the younger samples from these features. FS16 samples have grass pollen in concentrations similar to unit 3 at the base of trench 7 (Cummings, 1999). However, unit 3 has greater concentrations of *E. torreyana*–type pollen than *E. nevadensis*–type pollen, as do samples from unit 2 in trenches 2 and 3 (Cummings, 1999), in contrast to all samples from trench 7 (Fig. 8).

The differences between these *Ephedra* pollen occurrences at Hamburger Rock could be related to microclimate and depositional setting in an area near the limit of penetration of the summer monsoon (Shafer, 1989) and transitional between areas dominated by *E. nevadensis* and by *E. torreyana*. Trench 7 is located in the drainageway, which should retain moisture longer than the adjacent uplands with thin eolian sand mantling bedrock where the other trenches were dug. Alternatively, differences in wind direction and pollen transport may influence the relative proportions of *Ephedra* species.

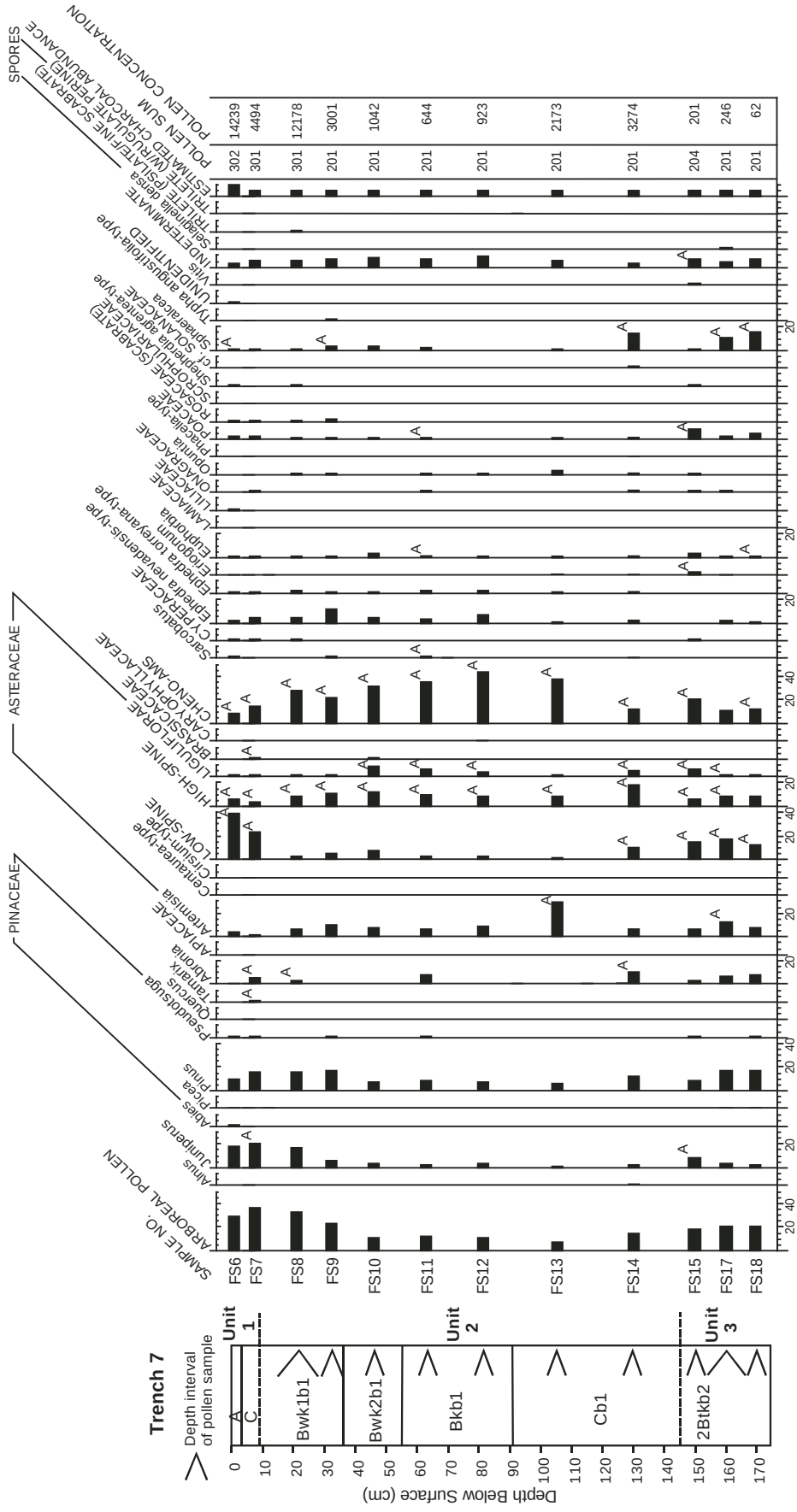

Figure 8. Results of pollen analysis with depth in trench 7 at Hamburger Rock (Cummings, 1999). Bracket adjacent to soil horizon designation shows thickness of sediment integrated in, for example, sample FS8. Notation "A" in columns represents presence of pollen grain aggregates, indicating proximity of a plant to the study site.

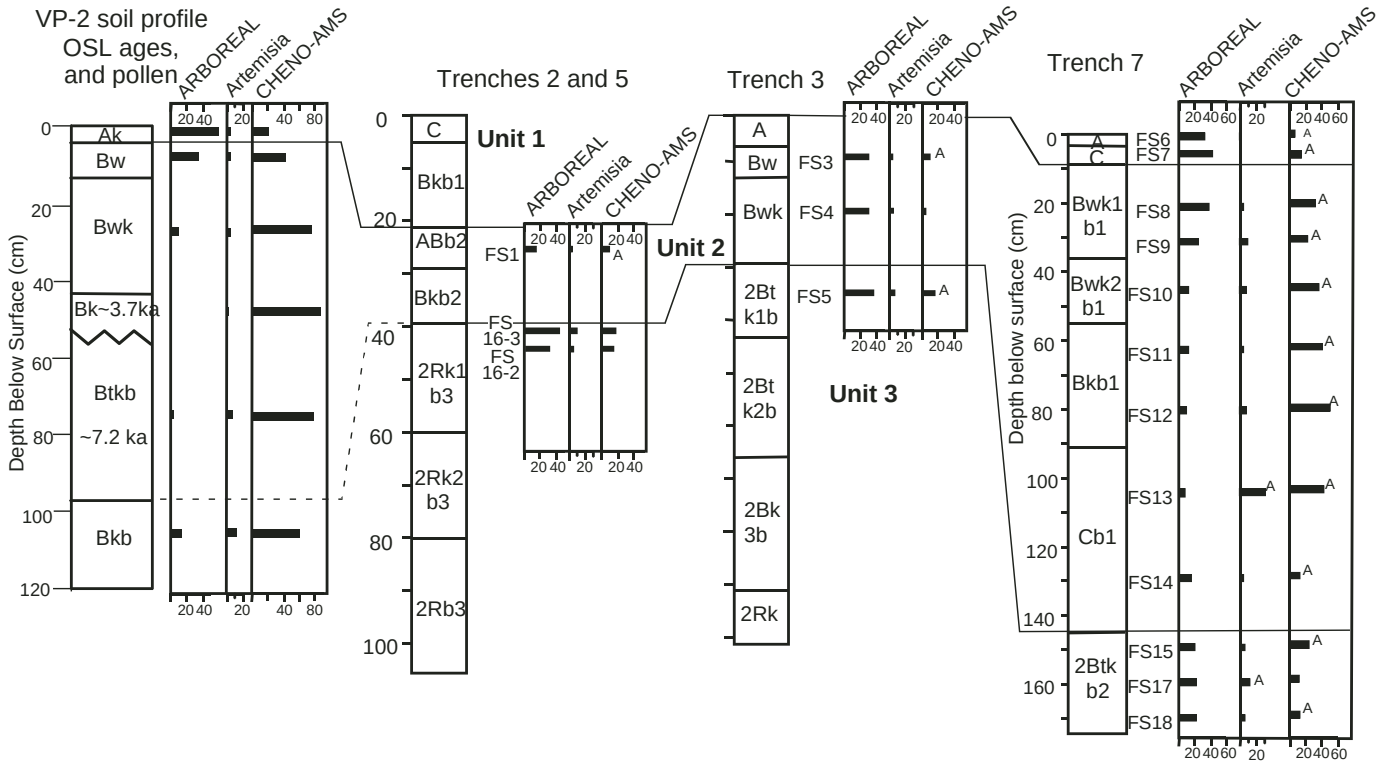

Figure 9. Summary of pollen data from soil pit VP-2 at Virginia Park site (complete data in Table DR4 [see footnote 1]) and trenches 2, 3, 5, and 7 at Hamburger Rock (Cummings, 1999), and correlation of pollen data, stratigraphic units, and paleosols among sites. Coarse-grained optically stimulated luminescence (OSL) ages shown for VP-2. Samples FS16-3 and -2 from trench 5 plotted at equivalent stratigraphic depth in trench 2; actual depths are 25 and 33 cm, respectively.

Sediment samples FS1, FS3, and FS4 are from the surface and buried soils formed on eolian unit 2 in trenches 2 and 3 (Fig. 9). They are similar to each other and to samples from 40 to 20 cm in trench 7 (except the difference in *Ephedra* types discussed above) containing abundant arboreal pollen with equal amounts of pollen from juniper and pine and less sagebrush pollen than older samples from trenches 2 and 3.

Pollen frequencies in samples from the dune-swale pit VP-2 (Fig. 9; see Table DR4 for species data [see footnote 1]) at Virginia Park reveal a similar record of climate and vegetation change. The lowermost sample (110–115 cm depth, or 20–25 cm below the coarse-grained OSL age of 7.7 ka) contains abundant grass and common arboreal pollen (13% *Pinus* and *Juniperus*) and *Artemisia* (11%). The middle part of the record, from 45 to 95 cm depth, is characterized by very high Cheno-Am percentages (~80%) and little or no arboreal pollen. The lowest arboreal pollen percentages and lowest *Artemisia*:Cheno-Am ratio are at the base of the surface soil, just below the coarse-grained OSL age of 4.2 ± 0.2 ka. *Pinus* and *Juniperus* increase greatly from below 14 cm depth to the surface, accompanied by a doubling of the *Artemisia*:Cheno-Am ratio. As noted above, the presence of pollen from the nonnative *Tamarix* in the Bw horizon (5–14 cm; Table DR4 [see footnote 1]) suggests that the uppermost sediments in the dune swale are less than 100 yr old, although burrowing may have mixed these surface sediments.

We correlate units between the two study sites as follows. The oldest eolian and fluvial sediment (unit 3) at Hamburger Rock has more arboreal and grass pollen and likely reflects wetter conditions than present. The paleosol properties suggest a correlation to eolian sand at the base of profile VP-2 (below the OSL age of 7.7 ± 0.3 ka), which also has more grass and arboreal pollen than younger samples, and to ca. 12–14 ka sand in dune-crest sites; thus, the oldest sediments at Hamburger Rock may be no younger than ca. 8 ka and as old as 12 ka. In addition, comparison of soil properties by profile development index values (Harden and Taylor, 1983) support correlations among the surface soils at VP-1, VP-2, and the accreting sheetwash soil in trench 7, and between soils on eolian unit 2 in trenches 2 and 3.

DISCUSSION AND REGIONAL SIGNIFICANCE

The relations between eolian and alluvial deposits and paleosols in Canyonlands and the paleoclimatic conditions during their formation can be compared with existing late Quaternary records from the Colorado Plateau (Fig. 1). We first discuss and compare the results of published studies of eolian deposits with those of the present study, followed by a brief comparison of alluvial records. We then discuss the broader implications of the timing of deposition of eolian and alluvial sediment to models of geomorphic response to climate change, and the nature and importance of rapid infiltration of dust to soils and vegetation communities.

Ages of Eolian Sand Deposits on the Colorado Plateau

The largest area of eolian sand in the southwestern United States is in the Four Corners region of the Colorado Plateau (Hack, 1941), which includes the Canyonlands area (Fig. 1). Despite the geographic extent of eolian deposits, published studies of their stratigraphy and soils are limited to the southern part of the region where dunes are less vegetated. Wells et al. (1990) found that dunes in the Chaco dune field of northwestern New Mexico (Fig. 1) were initially formed during the latest Pleistocene (ca. 16–12 ka) and were periodically

reactivated between ca. 6.5 and 2.8 cal ka and after 1.9 cal ka (Fig. 10). They interpreted the distribution and properties of surface and buried soils in the dune field to indicate relatively rapid pedogenesis by infiltration of eolian dust during periods of regional climate conditions that stabilized the dunes. The Tusayan dune field in northeastern Arizona (Fig. 1) has been repeatedly active during the Holocene (Fig. 10). Stokes and Breed (1993) suggested at least three phases of reactivation of Pleistocene linear dunes at ca. 4.7, 3–2, and 0.4 ka. Preliminary work by Anderson et al. (2001) indicated periods of eolian activity >10.4 to <9.2, <8.5 to >4.8, and ca. 4.0–2.8 cal ka. They suggested that Holocene periods of eolian activity alternating with shorter intervals of stability and pedogenesis varied with location rather than being of regional extent. Ellwein (1997) inferred periods of eolian activity before 100 ka, in latest Pleistocene to early Holocene time, and during the late Holocene on the southeastern edge of the Tusayan dune field.

The dune sands of the Four Corners region are presently mostly stable or partially active under grasses and shrubs, although the drought that began in 2001 may destabilize larger areas (Hiza, 2002). A dune mobility index (Lancaster, 1988) indicates that the dunes would be mostly active under meteorological conditions like those during the 1899–1904 drought (Muhs and Been, 1999). Since 1980, sand transport is regularly observed during most seasons at a monitoring station on the southwest margin of the Colorado Plateau (Helm and Breed, 1999).

In the present study, periods of eolian activity in the Canyonlands area correspond in a general way with those reported from other areas in the Colorado Plateau, but there are differences in details where age controls are more precise. The 46 ka eolian sand unit at Virginia Park is the oldest well-dated dune sand on the Plateau.

Eolian sand of late Pleistocene age (18–12 ka) in the Canyonlands area overlaps with a single radiocarbon age of ca. 15 cal ka from the Chaco dune field (Fig. 10). Wells et al. (1990) suggested that this period of dune formation extended from before this date to some time after, noting a reported age of ca. 19 cal ka on bone at the base of a loess unit near Monticello (Price et al., 1988). However, loess deposition need not coincide with sand deposition, especially where the loess appears to be derived from fluvial sediment of the San Juan River (Price et al., 1988), whereas the sand is locally derived. In the ISKY dune, two periods of sand transport separated by as much as 4000 yr of stability and pedogenesis occurred during 18–12 ka.

The timing of eolian deposition during the Holocene varies among Colorado Plateau sites. Eolian deposition at Virginia Park between ca. 9 and 7.5 ka coincides with a well-dated period of sand deposition at Cowboy Cave (Fig. 10; Lindsay, 1980; Spaulding and Petersen, 1980), and overlaps with sand deposition in the Tusayan dunes (Anderson et al., 2001). However, no early Holocene ages have been obtained in the Chaco dune field. The Chaco (Wells et al., 1990) and Tusayan dunes were locally active throughout the middle to late Holocene and Cowboy Cave experienced episodic sand deposition (Lindsay, 1980). In contrast, our results indicate only minor eolian deposition in the middle Holocene, including sheet sand at Hamburger Rock and in a swale at Virginia Park. Dunes were locally active in the Canyonlands area during the late Holocene up to the present day, as is the case elsewhere on the Colorado Plateau.

Alluvial Records

Many studies have addressed Quaternary fluvial history on the Colorado Plateau (e.g., Richmond, 1962; Harden and Colman, 1988; Love and Gillam, 1991; Hereford, 2002). Prominent gravel terrace remnants (Beaver Basin Formation) in Indian Creek and in Spanish Valley, near Moab (Fig. 1), are assigned to the 25–15 ka Pinedale glacial period of the Rocky Mountain region on the basis of degree of soil development and height above present stream level (Harden and Colman, 1988). Longpre (2001) reported deposition of a fluvial terrace in southeastern Utah between >13 ka to ca. 11 ka. Holocene deposits of sand and silt with local lenses of pebbles and gravels underlie major fill terraces and associated inset cut terraces along many modern stream channels. Episodes of fluvial aggradation and arroyo incision during the Holocene are well documented elsewhere on the Colorado Plateau (e.g., Hall, 1977; Karlstrom, 1988). Hereford (2002) interpreted fluvial deposits on the southern Colorado Plateau to indicate three major periods of valley alluviation separated by periods of arroyo cutting or channel adjustments during the past 2000 yr; he attributed these fluctuations to changes in flood frequency caused by climatic variations possibly related to El Nino-Southern Oscillation fluctuations.

Biggar and Adams (1987) reported ages of alluvial deposits in the Canyonlands area, including difficult-to-interpret radiocarbon and thermoluminescence ages on sediment in The Grabens area of Canyonlands National Park and in the Salt Creek drainage. Our OSL ages from site 9U-21 indicate deposition of mainly colluvial deposits, with minor fluvial reworking, at around 39 ka, 28 ka, and 16 ka (Table 4 and Fig. 10). Biggar and Adams (1987) report three ^{14}C ages between 4.2 and 2.8 cal ka on young graben-fill deposits at other sites. However, the ages of graben-fill deposits could reflect local events in the periodic filling of closed depressions that are not closely linked to paleoclimate.

Biggar and Adams (1987) interpreted the lower sediments in an 8-m-thick section along Salt Creek (Fig. 1) to represent sustained stream flow and the upper sediments, above a slight unconformity, to represent channeling and episodic high-discharge flows and occasional debris flows. Numerous radiocarbon ages on charcoal did not separate these phases chronologically, possibly as a result of old charcoal being reworked into young sediments (Biggar and Adams, 1987). They inferred that the alluvial sediments along Salt Creek were deposited between 2.5 and 2.0 cal ka and possibly as late as 0.5 cal ka. These conventional ages are consistent with our two AMS ages of ca. 1.8 cal ka on charcoal near the top of the same sequence (Fig. 4, Table 3).

In summary, the OSL ages from the present study suggest at least two alluvial sedimentation events before the last full-glacial period, but none during the full-glacial period of 28–20 ka (Figs. 3B and 10). Alluvial deposition in The Grabens resumed at ca. 16 ka and may have continued to as late as ca. 9 ka (Biggar and Adams, 1987); this episode may overlap with deposition of the Beaver Basin Formation along glaciated drainages (Harden and Colman, 1988). Middle Holocene sedimentation is recorded both in The Grabens (Biggar and Adams, 1987) and by the 5.3–cal ka alluvial deposit channeled into eolian sand at section 8U-13 at Virginia Park (Fig. 6). Rapid sedimentation at Salt Creek from ca. 2.5 cal ka to 1.9 cal ka culminated before the end of alluviation in the southern Colorado Plateau as reported by Hereford (2002).

Paleoclimate Records and Interpretations

Pollen data, stratigraphy, and soils at the Virginia Park and Hamburger Rock sites indicate significant changes in paleoclimate in the late Pleistocene and Holocene. These results can be compared with previous reconstructions of past climate in the Colorado Plateau that used pollen and plant macrofossils (Fig. 10). However, the wide range in local relief and seasonality of climate, the near absence of continuous records such as pollen from lake cores, and the highly localized nature of packrat middens (shady, frequently relatively moist alcoves) complicate correlations to other areas and to geomorphic records.

Few paleoclimate records exist for periods before 15 ka on the Colorado Plateau. Evidence from sparse lake cores and packrat middens (summarized by Wigand and Rhode, 2002) suggests that northern and central Utah was cold

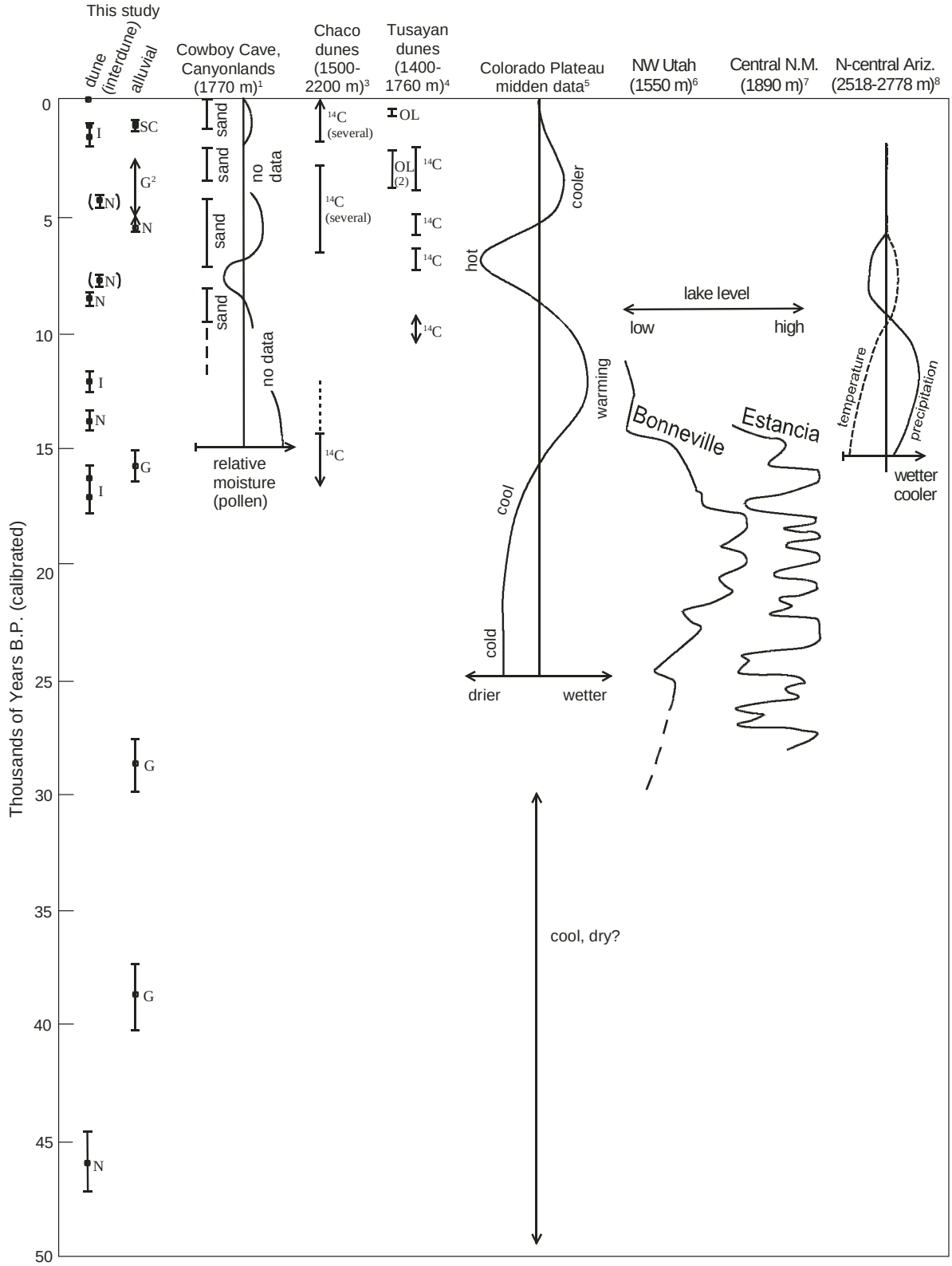

Figure 10. Timing of late Quaternary depositional events in Canyonlands area compared with other dated eolian sequences and paleoclimate records. V—Virginia Park site; I—ISKY site; G—graben-fill site; SC—Salt Creek site. Letters represent source of age control. ^{14}C—radiocarbon; OSL—optically stimulated luminescence. References: 1, Lindsay (1980), Spaulding and Peterson (1980); 2, Biggar and Adams (1987); 3, Wells et al. (1990); 4, Anderson et al. (2001), Stokes and Breed (1993); 5, Betancourt (1990), Sharpe (1991); 6, Oviatt and Miller (1997); 7, Allen and Anderson (2000); 8, Weng and Jackson (1999). All radiocarbon ages and ^{14}C-based curves from cited references were calibrated to calendar years by the CALIB program (Stuiver et al., 2003) to compare with OSL ages.

and dry from ca. 45 ka to 28 ka, coincident with low levels of Lake Bonneville (Fig. 10; Oviatt and Miller, 1997). During the transition to full-glacial conditions at ca. 25 ka, increased effective moisture (the balance between precipitation and evaporation) is indicated by shifts from sagebrush steppe to woodland (Wigand and Rhode, 2002) and rising levels of pluvial lakes (Oviatt and Miller, 1997; Allen and Anderson, 2000). However, midden data suggest this period remained relatively dry in southeast Utah (Betancourt, 1990; Sharpe, 1991). From ca. 20 ka to 15 ka, plant macrofossils suggest cooler and wetter conditions than present (Betancourt, 1990; Sharpe, 1991).

During the latest Pleistocene and early Holocene, precipitation increased (Fig. 10) because of the strengthening of the southwesterly summer monsoon (e.g., Shafer, 1989; Betancourt, 1990; Sharpe, 1991; Weng and Jackson, 1999). In a regional comparison of pollen records, Shafer (1989) showed that the ratio of *Artemisia* to Cheno-Am pollen increased sharply during this period, reflecting increased summer moisture. Effective moisture may have remained relatively stable during this period despite increasing temperatures, but runoff and sediment transport should have increased as a result of increased rainfall intensities associated with monsoon thunderstorms (Bull, 1991, p. 112–114). Destabilized surfaces accompanying changes in vegetation communities may also have increased sediment availability. Eolian deposits in our study area (14–8 ka) contain abundances of grass and arboreal pollen that are consistent with these regional records of wetter conditions than present.

Interpretations of paleoclimate and especially the relative strength of the summer monsoon suggest geographic and altitudinal variation across the Colorado Plateau during the early to middle Holocene (Fig. 10). Data from pollen and packrat middens indicate that the monsoon influence at altitudes similar to those of the present study began to wane by around 9 cal ka and reached a minimum at around 6.8 cal ka, followed by a period of maximum aridity (Shafer, 1989; Betancourt, 1990). At higher altitudes in southwestern Colorado, pollen and plant macrofossil records suggest that monsoonal influence continued into the late Holocene (Friedman et al., 1988; Petersen, 1988; Betancourt, 1990; Carrara et al., 1991; Sharpe, 1991).

From 8 ka to <4 ka, overlapping the proposed period of maximum aridity, we interpret relatively dry conditions dominated by summer rainfall in the Canyonlands area. In soil pit VP-2, the lowest arboreal pollen percentages and lowest *Artemisia*:Cheno-Am ratio are coincident with the transition from accretionary paleosol to overlying younger deposit, the base of which has an OSL age of 4.2 ± 0.2 ka (Fig. 9). Similar pollen trends appear in the thick sheetwash deposit (145–37 cm depth in trench 7) at Hamburger Rock.

The youngest sediment at Hamburger Rock and Virginia Park, including the uppermost 10 cm of trench 7, unit 1 in trench 2, and the uppermost 10 cm of VP-2, show an increase in arboreal pollen and a decrease in Cheno-Am pollen, recording increased effective moisture and, at Hamburger Rock, renewed eolian activity. These deposits represent the last several hundred to a thousand years and in part are of historic age, as indicated by the presence of tamarisk pollen. Part of the increase in arboreal pollen may reflect relatively recent invasion of *Juniperus* due to changes in land use, but climate change is supported by the concurrent increases in *Pinus* and *Picea* at both sites (Fig. 8 and Table DR4 [see footnote 1]).

Cowboy Cave, west of the Green River–Colorado River confluence, is the closest locality to the Canyonlands study sites that lie at a similar altitude. The stratified paleoclimate record from this cave (Fig. 10) indicates increased moisture from an enhanced monsoon from ca. 14 cal ka to 9 cal ka, followed by onset of drier conditions at ca. 9 cal ka (Spaulding and Petersen, 1980). By ca. 7.5 cal ka and extending to the present, relative moisture levels fluctuated (Lindsay, 1980). Similar to results of the present study, some periods of eolian sand deposition occurred during wetter intervals: >12 cal ka to ca. 9 cal ka, ca. 7–4 cal ka, and 1.3 cal ka to present.

The vegetation changes recorded in dated sediments from our study sites match well with records of latest Pleistocene through Holocene climatic changes on the Colorado Plateau (Fig. 10). Although limited in detail, our pollen data are derived from eolian and fluvial sediments and paleosols that permit direct association of these climatic changes with landscape response.

Timing and Episodic Nature of Dune Deposition, Alluviation, and Soil Formation

Records from a monitoring station in the Tusayan dune field (Helm and Breed, 1999) show that winds at this site have drift potentials (ability to move eolian sand) among the highest reported worldwide (Fryberger and Dean, 1979). These and other wind data coupled with measured ratios of precipitation to evapotranspiration in the Colorado Plateau (Muhs and Been, 1999) indicate that the region is extremely susceptible to wind erosion and sand transport. Thus, eolian activity is probably not transported-limited now or in the past; it is more likely that episodic sand deposition is caused by changes in sand supply from sediment sources or by changes in vegetation.

Comparison of the regional paleoclimate data and our local pollen data with dated eolian and alluvial deposits (Fig. 10) indicates eolian deposition occurred during relatively dry periods (8–6 ka, 2 ka to present) and also coincided with alluvial deposition during relatively wet periods (15–12 ka, 5–2 ka). Instead of a direct response to climate, the key factors for eolian activity in this region may be sediment production by weathering of sand particles from sandstone bedrock coupled with either sufficient moisture to produce runoff, or a drought sufficient to reduce or change the distribution of vegetation. Although closely linked eolian and fluvial deposition may seem counterintuitive, the relationship could be driven by greater sediment availability. During climatic transitions, the change or destabilization of vegetation could encourage transport of eolian sand as well as produce more available sediment on slopes. Such sediment is readily moved into drainages, but may not be transported far and ultimately could aggrade valley floors (Etheredge et al., 2004). Hereford (2002) attributes late Holocene aggradation in southern Colorado Plateau drainages to a long-term decrease in the frequency of large floods of high sediment transport capacity.

Evidence for eolian sand transport and deposition in the Colorado Plateau is lacking between ca. 45 ka and 18 ka, whereas episodic fluvial deposition is inferred from terraces along the Green and Colorado Rivers and drainages of the La Sal and Abajo Mountains (Harden et al., 1985) and recorded locally within The Grabens (Fig. 10). Interpretations of packrat midden data show that the climate in this region was relatively cold and dry before and during the full glacial (Betancourt, 1990; Oviatt and Miller, 1997; Allen and Anderson, 2000; Wigand and Rhode, 2002). Most paleoclimate interpretations suggest that the full-glacial period in the Colorado Plateau experienced little or no summer precipitation as monsoonal thunderstorms. Either such conditions were not conducive to production of sand by weathering, there was little runoff, and (or) the vegetation cover was sufficient to stabilize the sand produced. Because physical weathering during such glacial climates should have enhanced sand production from bedrock sources, some combination of the latter two explanations seems most likely. In addition to the apparent absence of eolian sand deposition, the low IRM values for paleosols indicate that atmospheric dust inputs were not significant during the period before ca. 17 ka.

The increase in precipitation and temperature during the late glacial and deglacial periods

(18–12 ka) was accompanied by a shift toward summer monsoonal precipitation (Shafer, 1989; Betancourt, 1990; Sharpe, 1991), and this shift is directly associated with the most substantial period of eolian sand deposition in both the Canyonlands area and the Chaco dune field (Fig. 10; Wells et al., 1990), as well as alluvial deposition in The Grabens. Along major drainages, late Pleistocene gravel terraces presumably correspond with this period, although very few numerical ages exist (Love and Gillam, 1991). The change in vegetation during this climate shift likely destabilized surface sediments, which were probably thick and abundant because of accelerated physical weathering during glacial climates, and the increase in runoff caused by more abundant and likely more intense summer rains increased fluvial transport and deposition. Both of these processes would have increased the sand supply, leading to both dune deposition and alluviation. In addition, the atmospheric dust supply apparently increased during this period, judging from the concentrations of magnetic silts in paleosols (Figs. 5 and 6).

Sand deposition, both eolian and fluvial, apparently stopped in the Canyonlands area by ca. 12 ka and a period of surface stabilization ensued, accompanied by rapid pedogenesis. The paleosols formed on unit 2 of the graben fill, unit 3 of the ISKY dune (Fig. 3), and the upper paleosol in dune-crest Virginia Park sites (Figs. 5 and 6) are all more strongly developed than those formed on older or younger late Pleistocene units, yet formed in a period as short as 4000 yr. At Hamburger Rock, the deepest paleosols in trenches 2, 3, and 7 (Fig. 7) probably also formed during this time. The soil properties document both rapid deposition of magnetic, far-traveled dust and sufficient moisture to translocate clays and $CaCO_3$ downward to form argillic and calcic horizons, and pollen data indicate relatively wet conditions (Figs. 8 and 9). These data corroborate similar results in the Chaco dune field (Wells et al., 1990) and are consistent with the presence of warmer, relatively wet conditions (compared with last glacial maximum) during the latest Pleistocene to early Holocene (Fig. 10) recorded throughout the region.

A brief period of eolian deposition at ca. 8 ka is recorded at Virginia Park, coincident with a decrease in rainfall and the appearance of drought-tolerant vegetation as the temperatures continued to warm (Fig. 10; Petersen, 1988; Shafer, 1989; Betancourt, 1990). This period corresponds with eolian deposition at Cowboy Cave (Spaulding and Petersen, 1980) and in the Tusayan dune field (Anderson et al., 2001). There are no dates indicating eolian sand deposition in the region during the height of the early to mid-Holocene drought, from ca. 7.5 ka to 6 ka, except for one site in the Tusayan dunes (Fig. 10). Comparison of properties of paleosols formed during this hiatus, which lasted 3000–4000 yr at our study sites, to those formed during the previous hiatus indicates that infiltration of eolian dust was greatly reduced during the younger period; the younger soils lack argillic horizons and exhibit weak (stage 1) secondary $CaCO_3$. These properties are consistent with relatively dry conditions indicated by climate records, as well as with the decrease in arboreal pollen and increase in Cheno-Am pollen at our sites.

Eolian and fluvial deposition resumed in the Canyonlands National Park area during a somewhat wetter, cooler period in the region beginning at ca. 6 ka and ending by ca. 3–2 ka (Fig. 10), as indicated by midden records (Betancourt, 1990; Sharpe, 1991) and pollen data (Lindsay, 1980; Petersen, 1988). Wells et al. (1990) note a brief hiatus accompanied by weak pedogenesis in the Chaco dune field at ca. 2.5 ka. Episodic eolian deposition in all three dune fields resumed by ca. 2 ka and continues to the present day.

CONCLUSIONS

The record of eolian and alluvial deposition in upland areas of the Canyonlands area reflects changes in climate and sediment availability during the past 50,000 yr. Paleosols formed during periods of landscape stability also record changes in local climate and regional conditions responsible for the production and delivery of eolian dust. Comparison of regional paleoclimate data and pollen data from the present study with episodes of deposition shows that eolian sand deposition occurred during both relatively wet periods and dry periods, whereas alluvial deposition occurred mostly during wetter periods. The apparent concurrence of eolian and alluvial deposition during relatively wet periods may result from increased sediment availability due to vegetation changes and to runoff from summer storms.

An important result of this study is that the delivery and soil-infiltration rate of magnetic, nutrient-rich eolian dust (Reynolds et al., 2001; Sanford et al., 2001) appears to have been at a maximum between ca. 12 and 8 ka. Before ca. 17 ka, and apparently back to at least 40 ka, little infiltrated dust is recorded in the paleosols. After ca. 8 ka, either the supply of dust was reduced or the more arid climate inhibited translocation of dust into the soils. These dust-enriched paleosols, which are within rooting distance of plants (50–100 cm depth), are important to plant nutrition and thus to the ecosystem as a whole (Belnap et al., 2000; Reynolds et al., 2001; Sanford et al., 2001). Recognition of the shallow depth and age of these paleosols, coupled with the ease with which they can erode when stabilizing crusts and vegetation are degraded (Belnap, 1995; Belnap and Gillette, 1997), is thus important to making land-management decisions in a time of fluctuating climate.

ACKNOWLEDGMENTS

Many people contributed their skills and strong backs to the collection and analysis of these samples. We thank Rich Tigges for assistance in augering samples; Eric Fisher for sediment analyses; Jeff Honke for preparation of pollen samples from Virginia Park; Jiang Xiao for magnetic-property analyses; Paul Lamothe for ICP-MS analyses; Mark Miller for vegetation descriptions in Virginia Park; Jack McGeehin for ^{14}C ages; and the Bobby's Hole crew for helping to carry samples and for general camp cheer. Many stimulating discussions with colleagues have contributed greatly to our understanding of the results presented here; we especially thank Mark Miller, Jayne Belnap, and Jason Neff. Thanks to Dan Muhs, Bob Thompson, Vance Holliday, and Jim O'Connor for thorough reviews of the manuscript and helpful suggestions for improvement.

REFERENCES CITED

Aitken, M.J., 1998, An introduction to optical dating: London, Oxford University Press, 267 p.

Allen, B.D., and Anderson, R.Y., 2000, A continuous, high-resolution record of late Pleistocene climate variability from the Estancia basin, New Mexico: Geological Society of America Bulletin, v. 112, p. 1444–1458.

Anderson, K.C., Anderson, D.E., and Neff, L.T., 2001, Soil formation and eolian activity during the Holocene: Implications for landscape stability on the Kaibito Plateau, Navajo Nation, Arizona: New York, American Association of Geographers, 97th Annual Meeting, p. 23.

Belnap, J., 1995, Surface disturbances; their role in accelerating desertification: Environmental Monitoring and Assessment, v. 37, no. 1–3, p. 39–57.

Belnap, J., and Gillette, D.A., 1997, Disturbance of biological soil crusts: Impacts on potential wind erodibility of sandy desert soils in southeastern Utah: Land Degradation and Rehabilitation, v. 8, p. 355–362.

Belnap, J., Reynolds, R., Reheis, M., and Phillips, S.L., 2000, What makes the desert bloom? The contribution of dust and crusts to soil fertility on the Colorado Plateau, *in* McArthur, E.D., and Fairbanks, D.J., eds., Proceedings, Shrubland Ecosystem Genetics and Biodiversity [2000 June 13–15, Provo, Utah]: Ogden, Utah, U.S. Department of Agriculture, 22 p.

Betancourt, J.L., 1990, Late Quaternary biogeography of the Colorado Plateau, *in* Betancourt, J.L., et al., eds., Packrat middens: The last 40,000 years of biotic change: Tucson, University of Arizona Press, p. 259–292.

Biggar, N.E., and Adams, J.A., 1987, Dates derived from Quaternary strata in the vicinity of Canyonlands National Park, *in* Campbell, J.A., ed., Geology of Cataract Canyon and vicinity: Four Corners Geological Society, 10th Field Conference Guidebook, p. 127–136.

Billingsley, G.H., Block, D.L., and Felger, T.J., 2002, Surficial geologic map of the Loop and Druid Arch quadrangles, Canyonlands National Park, Utah: U.S. Geological Survey Miscellaneous Field Studies Map MF-2411, scale 1:24,000.

Birkeland, P.W., 1999, Soils and Geomorphology (third edition): New York, Oxford University Press, 430 p.

Bull, W.B., 1991, Geomorphic responses to climatic change: New York, Oxford University Press, 326 p.

Buurman, P., Pape, T., and Muggler, C.C., 1997, Laser grain-size determination in soil genetic studies: 1. Practical problems: Soil Science, v. 162, p. 211–218.

Carrara, P.E., Trimble, D.A., and Rubin, M., 1991, Holocene treeline fluctuations in the northern San Juan Mountains, Colorado, USA, as indicated by radiocarbon-dated conifer wood: Arctic and Alpine Research, v. 23, p. 233–246.

Cummings, L.S., 1999, Pollen analysis at site 42SA23136: Denver, Colorado, Paleo Research Labs Technical Report 99-65, 10 p.

Ellwein, A.L., 1997, Quaternary evolution of eolian landforms, soils, and landscapes of the Petrified Forest National Park, Arizona [M.S. thesis]: Albuquerque, University of New Mexico, 175 p.

Etheredge, D., Gutzler, D.S., and Pazzaglia, F.J., 2004, Geomorphic response to seasonal variations in rainfall in the southwest United States: Geological Society of America Bulletin, v. 116, p. 606–618.

Friedman, I., Carrara, P., and Gleason, J., 1988, Isotopic evidence of Holocene climatic change in the San Juan Mountains, Colorado: Quaternary Research, v. 30, p. 350–353.

Fryberger, S.G., and Dean, G., 1979, Dune forms and wind regime, *in* McKee, E.D., ed., Global Sand Seas: U.S. Geological Survey Professional Paper 1052, p. 137–170.

Hack, J.T., 1941, Dunes of the western Navajo country: Geographical Review, v. 31, p. 240–263.

Haggerty, S.E., 1976, Opaque mineral oxides in terrestrial igneous rocks, *in* Rumble, D., ed., Oxide minerals: Mineralogic Society of America Short Course Notes, v. 3, p. Hg101–Hg300.

Hall, S.A., 1977, Late Quaternary sedimentation and paleoecologic history of Chaco Canyon, New Mexico: Geological Society of America Bulletin, v. 88, p. 1593–1618.

Harden, D., and Colman, S.M., 1988, Geomorphology and Quaternary history of Canyonlands, southeastern Utah, *in* Holden, G.S., and Tafoya, R.E., eds., Geological Society of America Field Trip Guidebook: Professional Contributions—Colorado School of Mines, no. 12, p. 336–369.

Harden, J.W., and Taylor, E.M., 1983, A quantitative comparison of soil development in four climatic regimes: Quaternary Research, v. 20, p. 342–359.

Harden, D.R., Biggar, N.E., and Gillam, M.L., 1985, Quaternary deposits and soils in and around Spanish Valley, Utah, *in* Weide, D.L., ed., Soils and Quaternary geology of the southwestern United States: Geological Society of America Special Paper 203, p. 43–64.

Hayton, S., Nelson, C.S., Ricketts, B.D., Cooke, S., and Wedd, M.W., 2001, Effect of mica on particle-analysis using the laser diffraction technique: Journal of Sedimentary Research, v. 71, p. 507–509.

Helm, P.J., and Breed, C.S., 1999, Instrumented field studies of sediment transport by wind, *in* Breed, C.S., and Reheis, M.C., eds., Desert winds: Monitoring wind-related surface processes in Arizona, New Mexico, and California: U.S. Geological Survey Professional Paper 1598, p. 31–54.

Hereford, R., 2002, Valley-fill alluviation during the Little Ice Age (ca. A.D. 1400–1880), Paria River basin and southern Colorado Plateau, United States: Geological Society of America Bulletin, v. 114, p. 1550–1563.

Herrmann, L., Jahn, R., and Stahr, K., 1996, Identification and quantification of dust additions in peri-Saharan soils, *in* Guerzoni, S., and Chester, R., eds., The impact of desert dust across the Mediterranean: The Netherlands, Kluwer Academic Publishers, p. 173–182.

Hiza, M.M., 2002, Factors affecting dune mobility on the Navajo Nation, Arizona: Proceedings, Fifth International Conference on Aeolian Research and the Global Change and Terrestrial Ecosystems–Soil Erosion Network (Wind), July 22–25, 2002: Lubbock, Texas Tech University, p. 385–386.

Hunt, C.B., 1969, Geologic history of the Colorado River: U.S. Geological Survey Professional Paper 669, p. 59–130.

Huntoon, P.W., Billingsley, G.H., and Breed, W.J., 1982, Geologic map of Canyonlands National Park and vicinity, Utah: Utah, Canyonlands Natural History Association Moab, scale 1:62,500.

Karlstrom, T.N.V., 1988, Alluvial chronology and hydrologic change of Black Mesa and nearby regions, *in* Gumerman, G.J., ed., The Anasazi in a changing environment: New York, Cambridge University Press, p. 45–91.

King, J.W., and Channel, J.E.T., 1991, Sedimentary magnetism, environmental magnetism, and magnetostratigraphy: Reviews of Geophysics Supplement, p. 358–370.

Lancaster, N., 1988, Development of linear dunes in the southwestern Kalahari, southern Africa: Journal of Arid Environments, v. 14, p. 233–244.

Lindsay, L.M.W., 1980, Pollen analysis of Cowboy Cave cultural deposits, *in* Jennings, J.D., ed., Cowboy Cave: Salt Lake City, University of Utah Press, Anthropological Paper 104, p. 213–224.

Longpre, C.I., 2001, Late Quaternary alluvial geochronology and geomorphology of lower Comb Wash, San Juan County, Utah: Geological Society of America Abstracts with Programs, v. 33, no. 5, p. 59.

Love, D.W., and Gillam, M.L., 1991, Levels of alluvial deposits and basalt flows and their estimated ages along drainages of the Navajo and Acoma-Zuni sections of the Colorado Plateau, *in* Morrison, R.B., ed., Quaternary nonglacial geology, conterminous U.S.: Geological Society of America Decade of North American Geology, v. K-2, p. 391–397.

Machette, M.N., 1986, Calcium and magnesium carbonates, *in* Singer, M.J., and Janitzky, P., eds., Field and laboratory procedures used in a soil chronosequence study: U.S. Geological Survey Bulletin 1648, p. 30–32.

Martin, P.S., 1963, The last 10,000 years: A fossil pollen record of the American Southwest: Tucson, University of Arizona Press, 87 p.

McCave, I.N., and Syvitski, J.P.M., 1991, Principles and methods of geological particle size analysis, *in* Syvitski, J.P.M., ed., Principles, methods and applications of particle size analysis: New York, Cambridge University Press, p. 3–21.

McDonald, E.V., Pierson, F.B., Flerchinger, G.N., and McFadden, L.D., 1996, Application of a soil-water balance model to evaluate the influence of Holocene climate change on calcic soils, Mojave Desert, California, USA: Geoderma, v. 74, p. 167–192.

McFadden, L.D., and McAuliffe, J.R., 1997, Lithologically influenced geomorphic responses to Holocene climatic changes in the Southern Colorado Plateau, Arizona: A soil-geomorphic and ecologic perspective: Geomorphology, v. 19, p. 303–332.

McFadden, L.D., Wells, S.G., and Jercinovich, M.J., 1987, Influences of eolian and pedogenic processes on the origin and evolution of desert pavement: Geology, v. 15, p. 504–508.

McFadden, L.D., McDonald, E.V., Wells, S.G., Anderson, K., Quade, J., and Forman, S.L., 1998, The vesicular layer and carbonate collars of desert soils and pavements: Formation, age and relation to climate change: Geomorphology, v. 24, p. 101–145.

Muhs, D.R., and Been, J.M., 1999, Reactivation of stabilized sand dunes on the Colorado Plateau: U.S. Geological Survey, http://geochange.er.usgs.gov/sw/impacts/geology/sand (last accessed 01/24/05).

Murray, A.S., and Wintle, A.G., 2000, Luminescence dating of quartz using an improved single-aliquot regenerative-dose protocol: Radiation Measurements, v. 32, p. 57–73.

Oviatt, C.G., and Miller, D.M., 1997, New explorations along the northern shores of Lake Bonneville, *in* Link, P.K., and Kowallis, B.J., eds., Mesozoic to recent geology of Utah: Salt Lake City, Brigham Young University Geology Studies, v. 42, part II, p. 345–372.

Petersen, K.L., 1988, Climate and the Dolores River Anasazi: Salt Lake City, University of Utah Press, University of Utah Anthropological Papers 113, 152 p.

Prescott, J.R., and Hutton, J.T., 1994, Cosmic ray contributions to dose rates for luminescence and ESR dating: Large depths and long-term time variations: Radiation Measurements, v. 23, p. 497–500.

Price, A.B., Nettleton, W.D., Bowman, G.A., and Clay, V.L., 1988, Selected properties, distribution, source, and age of eolian deposits and soils of southwest Colorado: Soil Science Society of America Journal, v. 52, p. 450–455.

Rees-Jones, J., 1995, Optical dating of young sediments using fine-grain quartz: Ancient TL, v. 13, p. 9–13.

Reheis, M.C., Goodmacher, J.C., Harden, J.W., McFadden, L.D., Rockwell, T.K., Shroba, R.R., Sowers, J.M., and Taylor, E.M., 1995, Quaternary soils and dust deposition in southern Nevada and California: Geological Society of America Bulletin, v. 107, p. 1003–1022.

Reynolds, R., Belnap, J., Reheis, M., Lamothe, P., and Luiszer, F., 2001, Aeolian dust in Colorado Plateau soils: Nutrient inputs and recent change in source: Proceedings of the National Academy of Sciences of the United States of America, v. 98, no. 13, p. 7123–7127.

Reynolds, R.L., Neff, J., Reheis, M., Goldstein, H., and Lamothe, P., 2003, Distribution of aeolian dust determined from magnetic and chemical properties in surficial substrates of grassland and shrubland, central Colorado Plateau (Utah): Eos (Transactions, American Geophysical Union), v. 84, Fall Meeting Supplement, abstract B11F-06.

Richmond, G.M., 1962, Quaternary stratigraphy of the La Sal Mountains, Utah: U.S. Geological Survey Professional Paper 324, 135 p.

Sanford, R., Reheis, M., Hanson, K., and Reynolds, R., 2001, Phosphorus in soils of a cool-desert ecosystem: Dust inputs and land-use effects on erosion, Colorado Plateau, USA: Eos (Transactions, American Geophysical Union), v. 82, abstract B12C-0131.

Shachak, M., and Lovett, G.M., 1998, Atmospheric deposition to a desert ecosystem and its implications for management: Ecological Applications, v. 8, p. 455–463.

Shafer, D.S., 1989, The timing of late Quaternary monsoon precipitation maxima in the southwest United States [Ph.D. dissertation]: Tucson, University of Arizona, 234 p.

Sharpe, S.E., 1991, Late-Pleistocene and Holocene vegetation change in Arches National Park, Grand County, Utah and Dinosaur National Monument, Moffat County, Colorado [M.S. dissertation]: Flagstaff, Northern Arizona University, 95 p.

Shearin, N.S., Reheis, M., and Cummings, L.S., 2000, 42SA23136 test report and analysis results: Bureau of Land Management, Monticello Field Office, 39 p.

Simonson, R.W., 1995, Airborne dust and its significance to soils: Geoderma, v. 65, p. 1–43.

Spaulding, W.G., and Petersen, K.L., 1980, Late Pleistocene and early Holocene paleoecology of Cowboy Cave, *in* Jennings, J.D., ed., Cowboy Cave: Salt Lake City, University of Utah Press, University of Utah Anthropological Paper 104, p. 163–177.

Stokes, S., and Breed, C.S., 1993, A chronostratigraphic re-evaluation of the Tusayan Dunes, Moenkopi Plateau and southern Ward terrace, northeastern Arizona, *in* Pye, K., ed., The dynamics and environmental context of aeolian sedimentary systems: Geological Society [London] Special Publication 72, p. 75–90.

Stuiver, M., Reimer, P.J., and Reimer, R., 2003, CALIB radiocarbon calibration: http://radiocarbon.pa.qub.ac.uk/calib/ (last accessed 01/24/05).

Thompson, R., and Oldfield, F., 1986, Environmental magnetism: London, Allen & Unwin, 227 p.

Walsh, P., and Schultz-Ela, D.D., 2003, Mechanics of graben evolution in Canyonlands National Park: Geological Society of America Bulletin, v. 115, p. 259–270.

Wells, S.G., McFadden, L.D., and Schultz, J.D., 1990, Eolian landscape evolution and soil formation in the Chaco dune field, southern Colorado Plateau, New Mexico: Geomorphology, v. 3, p. 517–546.

Weng, C., and Jackson, S.T., 1999, Late glacial and Holocene vegetation history and paleoclimate of the Kaibab Plateau, Arizona: Palaeogeography, Palaeoclimatology, Palaeocology, v. 153, p. 179–201.

Wigand, P.E., and Rhode, D., 2002, Great Basin vegetation history and aquatic systems: The last 150,000 years, *in* Hershler, R., Madsen, D.B., and Currey, D.R., eds., Great Basin aquatic systems history: Washington, D.C., Smithsonian Institution Press, Smithsonian Contributions to the Earth Sciences 33, p. 309–368.

Manuscript Received by the Society 5 May 2004
Revised Manuscript Received 27 October 2004
Manuscript Accepted 21 November 2004

Printed in the USA